THERMODYNAMIC PROPERTIES OF POLYMERS

Introduction

The thermodynamic properties of macromolecules cover a broad field of materials science. As with any material, macromolecules are well described if two sets of information are available: structure and energetics. Each of the two information sets can be separated into a microscopic and a macroscopic part. The microscopic description deals with matter on an atomic scale and with sizes in the nanometer range, and the macroscopic description, on a phase or larger scale, with sizes larger than micrometers. The thermodynamic properties cover the macroscopic description of energetics. For full understanding, however, the connection to the microscopic description is needed, which is achieved through statistical thermodynamics (qv). Another link to the microscopic description is offered by the kinetics that can be observed macroscopically, but for its interpretation and understanding a microscopic-level model must be available.

For many years, the thermodynamic description of macromolecules lagged behind other materials because of the unique tendency of polymeric systems to assume nonequilibrium states. Most standard sources of thermodynamic data are, thus, almost devoid of polymer information (1–7). Much of the aversion to include polymer data in standard reference sources can be traced to their nonequilibrium nature. In the meantime, polymer scientists have learned to recognize equilibrium states and utilize nonequilibrium states to explore the history of samples. For a nonequilibrium sample it is possible, for example, to thermally establish how it was transferred into the solid state (determination of the thermal and mechanical history). More recently, it was discovered with the use of temperature-modulated differential scanning calorimetry (TMDSC) that within the global, nonequilibrium structure of semicrystalline polymers, locally reversible melting and crystallization processes are possible on a nanophase level (8).

Equilibrium thermodynamic data are presented here to provide a base on which to judge the material on hand. It must always, however, be kept in mind that the actual samples analyzed are often not in equilibrium. Particularly, semicrystalline samples are not fully crystalline, do not contain perfect crystals that melt at the equilibrium melting temperature, and do not phase separate or mix when the thermodynamics are favorable (9–11). Similarly, many data must still be questioned as to their closeness to equilibrium or to the perfection of their extrapolation to equilibrium.

Basic to the thermodynamic description is the heat capacity which is defined as the partial differential $C_p = (\partial H/\partial T)_{n,p}$, where H is the enthalpy and T the temperature. The partial differential is taken at constant pressure and composition, as indicated by the subscripts p and n, respectively; A close link between microscopic and macroscopic description is possible for this fundamental property. The integral thermodynamic functions include enthalpy H entropy S, and free enthalpy G (Gibbs function). In addition, information on pressure p, volume V, and temperature T is of importance (PVT properties). The transition parameters of pure, one-component systems are seen as first-order and glass transitions. Mesophase transitions, in general, were reviewed (12) and the effect of specific interest to polymers, the conformational disorder, was described in more detail (13). The broad field of multicomponent systems is particularly troubled by nonequilibrium behavior. Polymerization thermodynamics relies on the properties of the monomers and does not have as many problems with nonequilibrium.

The instrumentation for (14) is covered mainly by calorimetry (15), thermogravimetry (16), and (17,18). Calorimetry is categorized into adiabatic calorimetry, covering the temperature range from 10 to 400 K (19–21), and differential scanning calorimetry (DSC), covering the temperature range from 200 to 1000 K (22,23). Isothermal or close-to-isothermal calorimetry includes combustion, reaction, and dissolution calorimetry (24). Much information on thermal analysis is collected in the Proceedings of the International Confederation for Thermal Analysis and Calorimetry (ICTAC) (25), and the North American Thermal Analysis Society (NATAS) (26). The broad range of literature is abstracted selectively (27). The thermal characterization of polymeric materials was described for the first time in an extensive treatise covering many types of polymers and many techniques of Thermal Analysis (qv) (28).

Heat Capacities of Solids and Liquids

Heat capacity C_p is of importance not only for the evaluation of the integral thermodynamic properties, such as enthalpy, entropy, and free enthalpy (Gibbs function), but also for the precise separation of latent heats of transition from motional energies and for the determination of glass transitions (29). Experimentally, in the low temperature region (0–100 K), heat capacity measurements are dominated by adiabatic calorimetry. Above that region, DSC has gained increasing prominence. Typical precision of measurements is now $\pm 3\%$ in the temperature range above 10 K for both solid and liquid heat capacities, although modern methods of a temperature-modulated DSC may increase the precision to levels as high as

±0.1% by eliminating heat losses through measuring the change of the calorimeter response as a function of frequency response of the calorimeter (30).

Below 10 K, the heat capacity C_p, although of interest for the theory of motion, does not contribute much to the integral H at higher temperature. It is dependent on the physical state (crystalline, semicrystalline, or amorphous), whereas the C_p of solids, from about 50 K to the glass-transition temperature T_g, is largely independent of the physical structure.

The theory of the heat capacity of solids is well established (31). The heat capacity is largely of vibrational origin and to a great extent described by the harmonic oscillator approximation. Classifying the vibrations into skeletal and group vibrations is useful. The former are of relatively low frequency, strongly coupled, and represent the intra- and intermolecular vibrations of the chain molecules. The skeletal vibrations dominate the heat capacity in the low temperature region (<100 K). All efforts to calculate the intermolecular, skeletal vibrations from crystal-structure and force-constant data were unsuccessful in the past. Heat capacity measurements still provide the best means for evaluation of the low frequency, integral vibrational spectrum. The intramolecular skeletal vibrations are somewhat higher in frequency and are accessible in their upper frequency range through isolated-chain normal-mode calculations (32). Such calculations also permit the evaluation of the numerous group vibrations. After an approximate vibrational spectrum has been established, the heat capacity at constant volume can be calculated up to, and even above, equilibrium melting temperatures of the polymeric materials. Figure 1 shows the cumulative frequency spectrum of polyoxymethylene (POM), and Figure 2 illustrates the the corresponding heat capacity contributions of the skeletal and group vibrations (**D** and **C**, respectively) as well as the total C_v (**B**) and C_p (**A**) (for theta temperatures, see Table 1).

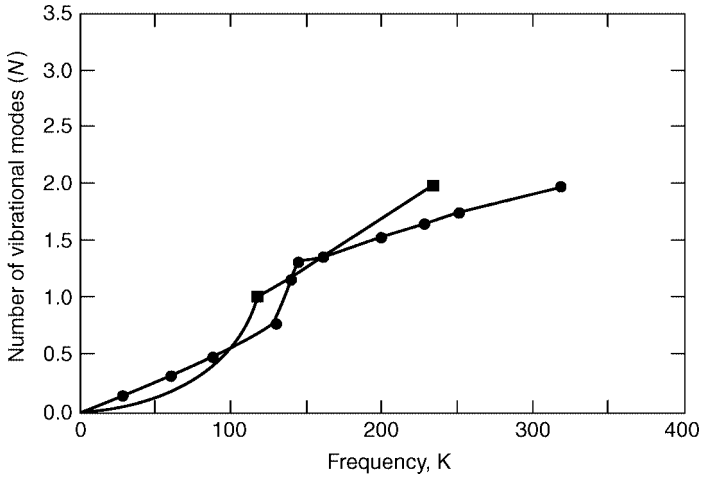

Fig. 1. Cumulative vibrational spectrum of the skeletal vibrations of polyoxymethylene (POM). ●, Experimental crystalline POM; ■, calculated with the Tarasov equation ($N = 2$).

Table 1. Thermal Properties of Linear Macromolecules[a]

	T_g	ΔC_p[b]	T_m	ΔH_f[c]	SHG[d]	S_0[e]	θ_1	θ_3	N[f]	C_p[g]
Poly(alkenes)										
Polyethylene [poly(methylene)]										
(c)	—	—	414.6	4.11	X	0	519	158	2	0.1–410
(a)	237	10.5(1)	—	—	X	3.0	519	80	2	0.1–600
Polypropylene										
(c)	—	—	460.7	8.70	X	0	714	91	7	10–460
(a)	270	19.2(2)*	—	—	X	5.2	633	78	7	10–600
Poly-1-butene										
(c)	—	—	411.2	7.00	X	0	618	93	9	10–249**
(a)	249	23.1(2)	—	—	X	6.4	618	(80)	9	249–630
Poly-1-pentene										
(c)	—	—	403.2	6.30	X	0	580	(93)	11	200–233**
(a)	233	27.0(2)	—	—	X	(0.9)	580	(80)	11	233–470
Poly-1-hexene										
(a)	223	25.1(2)	—	—	X	?	563	86	13	20–290
Polycyclopentene										
(a)	173	28.9(4)	—	—	X	?	582	88	10	10–320
Poly(4-methyl-1-pentene)										
(c)	—	—	523.2	9.96	X	0	660	(93)	14	80–303**
(a)	303	30.1(1+1)	—	—	?	?	660	?	14	303–540
Polyisobutylene										
(c)	—	—	317	12.0	X	0	850	?	10	?
(a)	200	21.3(2)	—	—	X	?	850	103	10	15–380
Poly(1-butenylene), *cis*										
(c)	—	—	284.7	9.20	X	0	589	87	8	30–171**
(a)	171	27.2(3)*	—	—	X	17.5	589	?	8	171–350
Poly(1-butenylene), *trans*										
(c)	—	—	437	3.73[h]	X	0	599	95	8	30–190**
(a)	190	28.0(3)*	—	—	X	16.2	599	?	8	190–500
Poly-1,4-(2-methyl-butadiene), *cis*										
(c)	—	—	301.2	4.35	?	0	647	(120)	1	?
(a)	200	30.9(3)	—	—	X	?	647	58	11	2–360
Poly(vinyl)s and Related Polymers										
Poly(vinyl alcohol)										
(c)	—	—	538	7.11	X	0	495	119	4	60–300**
(a)	358	?(2)	—	—	?	?	495	?	4	?
Poly(vinyl acetate)										
(a)	304	40.7(?)	—	—	X	?	600	(86)	11	80–370
Poly(vinyl fluoride)										
(c)	—	—	503.2	7.54	X	0	440	105	4	80–314**
(a)	314	17.0(2)*	—	—	X	9.4	440	?	4	480–530[i]
Poly(vinylidene fluoride)										
(c)	—	—	483.2	6.70	X	0	346	66	4	5–212**
(a)	212	21.2(2)*	—	—	X	5.1	346	?	4	450–580[i]
Polytrifluoroethylene										
(c)	—	—	495.2	5.44	X	0	315	56	4	25–280**
(a)	280	13.8(2)*	—	—	X	13	315	?	4	480–600[i]
Polytetrafluoroethylene										
(c)	—	—	605	4.10[j]	X	0	250	54	2	0.3–280[i]
(a)	200	9.4(1)	—	—	X	3.3	250	?	2	180–700

Table 1. (Continued)

	T_g	ΔC_p[b]	T_m	ΔH_f[c]	SHG[d]	S_0[e]	θ_1	θ_3	N[f]	C_p[g]
Poly(vinyl chloride)										
(a)	354	19.4(2)	—	—	X	2.4	354	45	4	5–380
Poly(vinylidene chloride)										
(c)	—	—	463	?	X	0	308	119	4	60–255**
(a)	255	?(2)	—	?		?	308	?	4	?
Poly(chlorotrifluoroethylene)										
(c)	—	—	493	5.02	X	0	215	42	4	1–325**
(a)	325	?(2)	—	—	?	?	215	?	4	?
Polystyrene										
(c)[k]	—	—	516.2	10.0	X	0	284	110	6	?
(a)	373	30.8(1+1)	—	—	X	4.4	284	48	6	0.1–600
Poly(α-methylstyrene)										
(a)	441	25.3(1+1)	—	—	X	?	450	48	9	1.4–490
Aliphatic Poly(oxide)s										
Poly(oxymethylene)										
(c)	—	—	457.2	9.79	X	0	232	117	2	0.1–390
(a)	190	28.2(2)*	—	—	X	3.4	232	?	2	190–600
Poly(oxyethylene)										
(c)	—	—	342	8.66	X	0	353	114	4	10–342
(a)	206	38.2(3)*	—	—	X	8.1	353	?	4	206–450
Poly(oxymethyleneoxyethylene)										
(c)	—	—	328	16.7	X	0	317	114	6	10–328**
(a)	209	62.1(5)*	—	—	X	27	317	?	6	209–390
Poly(oxytrimethylene)										
(c)	—	—	308	9.44	X	0	433	100	6	1.0–308
(a)	195	46.8(4)*	—	—	X	7.8	433	40	6	1.0–330
Poly(oxytetramethylene)										
(c)	—	—	330	14.4	X	0	436	90	8	5–189**
(a)	189	57.0(5)*	—	—	X	17	436	?	8	189–340
Poly(oxyoctamethylene)										
(c)	—	—	347	29.3	X	0	480	137	16	14–255**
(a)	255	83.1(9)*	—	—	X	63	480	?	16	350–360
Poly(oxymethyleneoxytetramethylene)										
(c)	—	—	296	14.3	X	0	392	122	10	10–296
(a)	189	83.8(7)*	—	—	X	15	392	?	10	189–360
Poly(oxypropylene)										
(c)	—	—	348	8.40	X	0	494	112	7	80–198**
(a)	198	32.1(3)*	—	—	X	9.4	494	?	7	198–370
Poly(acrylate)s and (methacrylate)s										
Poly(methyl acrylate)										
(a)	279	42.3(?)	—	—	X	?	552	86	11	10–500
Poly(ethyl acrylate)										
(a)	249	45.6(?)	—	—	X	?	543	89	13	90–500
Poly(*n*-butyl acrylate)										
(a)	218	45.4(?)	—	—	X	?	518	88	17	80–440
Poly(isobutyl acrylate)										
(a)	249	36.6(?)	—	—	X	?	(524)	(90)	18	230–500
Poly(methyl methacrylate)										
(c)	—	—	450	9.60	X	0	680	(140)	14	?
(a)	378	32.7(?)	—	—	X	7.1	680	67	14	0.2–550

Table 1. (Continued)

	T_g	ΔC_p[b]	T_m	ΔH_f[c]	SHG[d]	S_0[e]	θ_1	θ_3	N[f]	C_p[g]
Poly(ethyl methacrylate)										
(a)	338	31.7(?)	—	—	X	?	622	(60)	16	80–380
Poly(*n*-butyl methacrylate)										
(a)	293	27.9(?)	—	—	X	?	559	58	20	80–440
Poly(isobutyl methacrylate)										
(a)	326	39.0(?)	—	—	X	?	595	(60)	21	230–400
Polyacrylonitrile										
(a)	378	?(?)	—	—	X	?	980	62	6	60–370
Aliphatic Poly(ester)s										
Polyglycolide										
(c)	—	—	501	9.74	X	0	521	98	6	10–318**
(a)	318	31.8(2)	—	—	X	7.6	521	?	6	318–550
Poly(ethylene oxalate)										
(c)	—	—	450	23	?	0	533	?	12	?
(a)	306	56.2(4)	—	—	X	?	533	89	12	10–360
Poly(β-propiolactone)										
(c)	—	—	366	10.9	X	0	522	85	8	10–249**
(a)	249	42.9(3)	—	—	X	15.2	522	?	8	249–400
Poly(L-lactic acid)										
(c)	—	—	480	6.55	X	0	574	(52)	9	190–470**
(a)	332.5	43.8(2+1)	—	—	X	1.7	574	52	9	5.0–250
Poly(γ-butyrolactone)										
(c)	—	—	337.5	14.0	X	0	474	96	10	10–214**
(a)	214	52.0(4)	—	—	X	20.6	474	?	10	214–350
Poly(δ-valerolactone)										
(c)	—	—	331	18.8	X	0	502	101	12	10–207**
(a)	207	60.9(5)	—	—	X	32	502	?	12	207–350
Poly(ε-caprolactone)										
(c)	—	—	342.2	17.9	X	0	491	101	14	10–209**
(a)	209	67.4(6)	—	—	X	23	491	?	14	209–350
Polyundecanolactone										
(c)	—	—	365	39.5	X	0	528	105	24	10–227**
(a)	227	102.7(11)	—	—	X	68	528	?	24	227–400
Polytridecanolactone										
(c)	—	—	368	50.6	X	0	519	112	28	10–229**
(a)	229	115.8(13)	—	—	X	92	519	?	28	229–370
Polypentadecanolactone										
(c)	—	—	370.5	63.4	X	0	525	114	32	10–251**
(a)	251	124(15)	—	—	X	128	525	?	32	251–370
Poly(pivalolactone)										
(c)	—	—	513.0	14.8	X	0	585	(98)	14	150–267**
(a)	267	37.6(3)	—	—	X	16.5	585	?	14	267–550
Poly(butylene adipate)										
(c)	—	—	328.8	?	X	0	514	(108)	24	80–199**
(a)	199	140.0(?)	—	—	?	?	514	?	24	199–450
Poly(ethylene sebacate)										
(c)	—	—	356.2	31.9	X	0	514	(158)	28	120–245**
(a)	245	127.0(12)	—	—	X	(26)	514	(80)	28	245–410
Poly(dimethyl itaconate)										
(a)	377	54.2(?)	—	—	X	?	557	(67)	20	110–450

Table 1. (Continued)

	T_g	ΔC_p[b]	T_m	ΔH_f[c]	SHG[d]	S_0[e]	θ_1	θ_3	N[f]	C_p[g]
Poly(di-*n*-propyl itaconate)										
(a)	304	57.8(?)	—	—	X	?	428	(67)	28	110–410
Poly(di-*n*-heptyl itaconate)										
(a)	172[l]	45.6(?)	—	—	X	?	582	(67)	44	110–170
Poly(di-*n*-octyl itaconate)										
(a)	178[l]	99.1(?)	—	—	X	?	518	(67)	48	110–170
Poly(di-*n*-nonyl itaconate)										
(a)	187[l]	183.4(?)	—	—	X	?	589	(67)	52	110–180
Aliphatic Poly(amide)s										
Nylon 6										
(c)	—	—	533	26.0	X	0	544	(67)	14	70–313**
(a)	313	53.7(6)*	—	—	X	37	544	?	14	313–600
Nylon 11										
(c)	—	—	493	44.7	X	0	420	(67)	24	230–316**
(a)	316	68.4(11)*	—	—	X	78	420	?	24	316–550
Nylon 12										
(c)	—	—	500	48.4	X	0	455	(67)	26	230–314**
(a)	314	74.3(12)*	—	—	X	82	455	?	26	314–540
Nylon 6,6 α										
(c)	—	—	574	57.8	X	0	614	84	28	0.3–323**
(a)	323	115.5(12)*	—	—	X	77	614	?	28	323–600
Nylon 6,9										
(c)	—	—	500	69	X	0	579	(84)	34	230–331**
(a)	331	109.5(15)*	—	—	X	114	579	?	34	331–590
Nylon 6,10										
(c)	—	—	506	71.7	X	0	543	(84)	36	230–323**
(a)	323	118.0(16)*	—	—	X	120	543	?	36	323–590
Nylon 6,12										
(c)	—	—	520	80.1	X	0	533	(84)	40	230–319**
(a)	319	141.4(18)*	—	—	X	124	533	?	40	319–600
Polymethacrylamide										
(a)	?	?	—	—	X	?	523	(193)	10	60–300
Poly(amino acid)s										
Polyglycine II										
(c)	—	—	?	?	X	0	750	81	6	1.4–390**
Poly(L-alanine)										
(c)	—	—	?	?	X	0	634	58	9	1.6–390**
Poly(L-valine)										
(c)	—	—	?	?	X	0	664	65	14	2.0–390**
Poly(L-serine)										
(c)	—	—	?	?	X	0	685	(68)	10	220–390**
(a)	(400)[m]	(30.0)[m]	—	—	X	?	685	?	10	?
Poly(L-leucine)										
(c)	—	—	?	?	X	0	625	(68)	16	220–390**
Poly(L-aspartic acid) sodium salt										
(c)	—	—	?	?	X	0	597	(68)	14	220–390**
Poly(L-glutamic acid) sodium salt										
(c)	—	—	?	?	X	0	907	(68)	16	220–390**
Poly(L-phenylalanine)										
(c)	—	—	?	?	X	0	610	(68)	11	220–390**

Table 1. (Continued)

	T_g	ΔC_p[b]	T_m	ΔH_f[c]	SHG[d]	S_0[e]	θ_1	θ_3	N[f]	C_p[g]
Poly(L-tyrosine)										
(c)	—	—	?	?	X	0	729	(68)	13	220–390**
Poly(L-asparagine)										
(c)	—	—	?	?	X	0	569	(68)	12	220–390**
Poly(L-tryptophan)										
(c)	—	—	?	?	X	0	793	(68)	13	220–390**
Poly(L-proline)										
(c)	—	—	?	?	X	0	691	(68)	11	220–390**
Poly(L-lysine) hydrogen bromide										
(c)	—	—	?	?	X	0	636	(68)	20	220–390**
Poly(L-methionine)										
(c)	—	—	?	?	X	0	691	(68)	15	220–390**
(a)	(400)[m]	(61.0)[m]	—	—	X	?	691	?	15	?
Poly(L-histidine)										
(c)	—	—	?	?	X	0	808	(68)	13	220–390**
Poly(L-histidine) hydrogen chloride										
(c)	—	—	?	?	X	0	745	(68)	16	220–390**
Poly(L-arginine) hydrogen chloride										
(c)	—	—	?	?	X	0	610	(68)	23	220–390**
Phenylene Containing Polymers										
Poly(*p*-phenylene)										
(c)	—	—	>1000	?	X	0	544	(54)	3	80–300**
Poly(thio-1,4-phenylene)										
(c)	—	—	593	8.65	X	0	566	(54)	5	220–363**
(a)	363	29.2(0+1)	—	—	X	(4.2)	566	(40)	5	363–600
Poly(*p*-xylylene)										
(c)	—	—	700	10.0[n]	X	0	562	(54)	7	220–410**
(a)	286	37.6(1+1)*	—	—	?	?	562	(40)	7	(286–410)
Poly(oxy-1,4-phenylene)										
(c)	—	—	535	7.82	X	0	555	(54)	5	300–358**
(a)	358	21.4(0+1)	—	—	X	(10)	555	(40)	5	358–620
Poly(oxy-2,6-dimethyl-1,4-phenylene)										
(c)	—	—	580	5.95	X	0	564	(54)	5	80–482**
(a)	482[o]	31.9(1+1)	—	—	X	(7.5)	564	(40)	5	482–570
Poly(ethylene terephthalate)										
(c)	—	—	553	26.9	X	0	586	54	15	1.0–10
(a)	342	77.8(4+1)	—	—	X	22	586	44	15	1.0–590
Poly(trimethylene terephthalate)										
(c)	—	—	510	30.0	X	0	550	51	19	5.0–300**
(a)	315	94(5+1)	—	—	X	31.4	550	(51)	19	320–570
Poly(butylene terephthalate)										
(c)	—	—	518.2	32.0	X	0	542	(54)	19	150–310**
(a)	248[p]	107(6+1)	—	—	X	(10)	542	(40)	19	248–570
Poly(4-hydroxybenzoic acid)										
(c)	—	—	—	—[q]	X	0	823	(54)	7	170–434**
(a)	434	33.2(1+1)	—	—	X	?	823	(25)	7	—
Poly(2,6-hydroxynaphthoic acid)										
(c)	—	—	—	—[r]	X	0	640	(54)	9	170–399**
(a)	399	46.5(1+1)	—	—	X	?	640	(27)	9	399–650

Table 1. (Continued)

	T_g	ΔC_p[b]	T_m	ΔH_f[c]	SHG[d]	S_0[e]	θ_1	θ_3	N[f]	C_p[g]
Poly(ethylene-2,6-naphthalene dicarboxylate)										
(c)	—	—	610	25.0	X	0	600	(54)	17	220–390**
(a)	390	81.6(4+1)	—	—	X	(10)	600	(30)	17	390–600
Poly(4,4′-isopropylidene diphenylene carbonate)										
(c)	—	—	608.2	33.6	X	0	569	(54)	14	?
(a)	424	48.8(2+2)	—	—	X	25	569	40	14	0.4–750
Poly(oxy-1,4-phenylene-oxy-1,4-phenylene-carbonyl-1,4-phenylene)										
(c)	—	—	668.2	37.4	X	0	560	(54)	15	130–419**
(a)	419[s]	78.1(1+3)	—	—	X	(17)	560	(40)	15	419–680
Polysilylenes and Siloxanes										
Poly(dimethylsilylene)										
(c)	—	—	?	—[t]	X	0	342	(68)	8	160–490**
(a)	?	?	—	—	X	?	342	?	8	?
Poly(dipentylsilylene)										
(c)	—	—	?	—[u]	X	0	320	(68)	24	160–490**
(a)	227	71.3	—	—	X	?	320	?	24	?
Poly(dimethyl siloxane)										
(c)	—	—	219	2.75	X	0	509	68	10	8–146**
(a)	146	27.7(2)	—	—	X	3.5	509	?	10	146–340
Poly(diethyl siloxane)										
(c)	—	—	282.7	1.84[v]	X	0	480	87	14	10–135**
(a)	135	30.2(2)	—	—	X	8.4	480	?	14	135–360

[a]The glass-transition temperature is listed as T_g; ΔC_p is the change of the heat capacity at T_g for the fully amorphous sample; T_m is the equilibrium melting temperature; ΔH_f, the heat of fusion for the 100% crystalline sample; S, H, and G are the entropy, enthalpy, and Gibbs function, respectively; S_0 represents the residual entropy at absolute zero; θ_3 and θ_1 are the characteristic temperatures for the contributions of the skeletal vibrations to the heat capacity; N represents the number of skeletal vibrations per repeating unit (the total number of vibrations is given by the number of degrees of freedom = three times the number of atoms in the repeating unit); C_p denotes the heat capacity at constant pressure.

Data as of November 1994 (33); (a) represents the amorphous sample, and (c) the 100% crystalline; the mark ** represents heat capacities for a semicrystalline polymer. The continually updated full version of the data bank with tables and graphs can be accessed at the Internet over our Web page (34). The critically reviewed experimental data which provided the base for the data bank are available through References 35–44.

[b]The change in the heat capacity, listed in J/K · mol, at T_g as derived from the ATHAS recommended, experimental data. The mark * in this column indicates that the data were derived, instead, from the difference between experimental, liquid C_p and the calculated, solid C_p. The first numeral in parentheses refers to the number of small mobile beads that make up the repeating unit (such as CH_2—, O—, or $CHCH_3$—). The average increase in C_p at T_g of all listed molecules per small bead is 11.5 ± 1.7 J/K · mol. The second numeral refers to large beads (such as C_6H_4—). The increase in C_p of a large bead at T_g is double or triple that of a small bead.

[c]The melting temperature is the best estimate of the equilibrium melting temperature, and the heat of fusion in kJ/mol of repeating unit is computed for 100% crystallinity.

[d]An X in this column indicates that enthalpy, entropy, and Gibbs energy are available, on the basis of the ATHAS recommended data (34); ? indicates that the data is unknown.

[e]Residual entropy in the glassy state at zero temperature, in J/K · mol.

[f]The number of skeletal vibrational modes used in the Tarasov equation with the theta temperatures of the previous two columns. Values of theta temperatures in parentheses are estimates on the basis of data from polymers of similar backbone structure.

Table 1. (Continued)

[g] Temperature range of the ATHAS recommended experimental heat capacity data. The computations of heat capacities of solids are based on these data and are usually carried out from 0.1 to 1000 K, to provide sufficiently broad ranges of temperature for the addition schemes and for analysis of superheated polymers, as in laser ablation studies.
[h] The *trans*-PBUT has an additional condis state at lower temperature. The crystal–condis crystal transition is at 356 K, and the heat of transition is 7.8 kJ/mol (45,46).
[i] Between T_g and T_m, the C_p of the liquid cannot be extrapolated from melt since the liquid heat capacities of the fluorinated polymers are nonlinear.
[j] The PTFE has additional crystal–crystal–condis crystal transitions at 292 and 303 K; their combined heats of transition are 850 J/mol (47).
[k] For deuterated, amorphous, solid polystyrene and ring-only deuterated polystyrene, heat capacities lead to Tarasov θ_3 and θ_1 temperatures of 55, 244 K and 49, 278 K, respectively. The thermodynamic functions S, H, and G are found in Reference 48. For other data, see Reference 49.
[l] The listed glass-transition temperature has been assigned to relaxation processes of the n-alkyl side groups. The T_{gu} has been assigned to the backbone (44).
[m] The glass-transition and the ΔC_p in two amino acids PLSER and PLMET have been estimated for the main chain (50).
[n] The PPX has two lower first-order transitions, leading to condis crystals at 504 and 560 K with heats of transition of 5.0 and 1.5 kJ/mol (51).
[o] Semicrystalline PPO shows the existence of a rigid-amorphous phase which governs the thermal properties from T_g to T_m. Fusion, superheating, and annealing are directly affected by the rigid-amorphous phase (52).
[p] The glass-transition temperature of quenched PBT is 248 K, and the change in C_p at T_g is 107 J/K · mol. Semicrystalline PBT has a T_g at 310 to 325 K, and the change in C_p at 320 K is 77 J/K · mol. In addition, it shows existence of a rigid-amorphous fraction (53).
[q] The POB shows a disordering transition at 616.5 K with a heat of transition of 3.8 kJ/mol (54).
[r] The PON shows a disordering transition at 614.5 K with a heat of transition of 0.4 kJ/mol (54).
[s] Above T_g, poorly crystallized samples show a rigid–amorphous fraction that does not contribute to the increase in heat capacity at T_g (55).
[t] The PDMSi shows two small transitions. One is at 240 K with a heat of transition of 0.1 kJ/mol and the other at 432.5 K with a heat of transition of 0.56 kJ/mol is probably a transition from one crystal form to another (56).
[u] The PDPSi shows a disordering transition from condis crystal I to condis crystal II at 338.3 K with a heat of transition of 1.4 kJ/mol (56).
[v] The PDES has an additional condis state at a lower temperature. The crystal–condis crystal transition is at 206.7 K; its heat of transition is 2.72 kJ/mol (57).

The Einstein function (58) inverts frequency to heat capacity. Integrating the data of Figure 1 over all frequencies leads to the heat capacity

$$\frac{C_v}{NR} = \int_0^{\theta_{max}} \frac{(\theta/T)^2 \exp(\theta/T)}{[\exp(\theta/T) - 1]^2} \, d\theta \tag{1}$$

where T is the temperature and θ is the frequency, both expressed in kelvin ($\theta = h\nu/k$, with ν representing the frequency in Hz; h and k are Planck's and Boltzmann's constants, respectively; 1.0 Hz = 4.799×10^{-11} K, 1.0 cm^{-1} = 1.4388 K).

The integration of equation 1 is evaluated in steps for the various regions of the frequency distributions found for macromolecules. The lowest vibrational frequencies (skeletal) usually follow a quadratic function up to a frequency limit called θ_D or θ_3. This is the well-known Debye approximation (59) of the low temperature heat capacity at constant volume, C_v (**B**), which in this temperature range

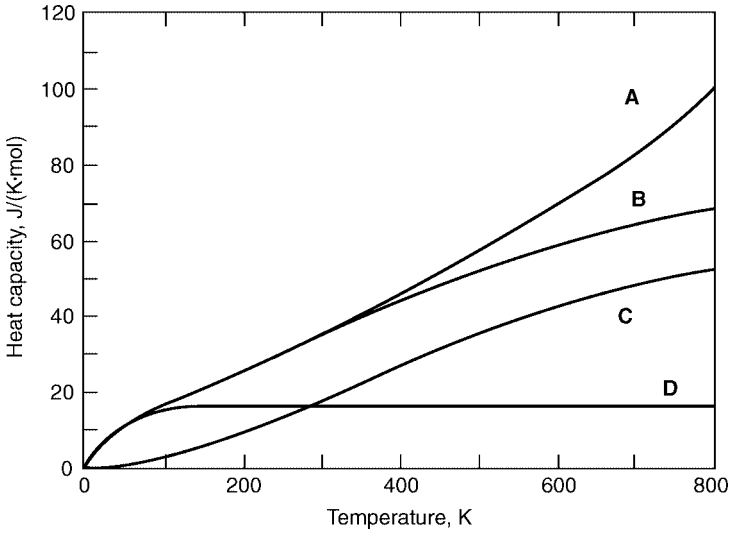

Fig. 2. Heat capacity contributions of the skeletal and group vibrations of solid polyoxymethylene, calculated by the Advanced Thermal Analysis System (ATHAS). **A**, C_p; **B**, C_v; **C**, group vibrations; **D**, skeletal vibrations. To convert J to cal, divide by 4.184.

is little different from C_p (**A**)

$$D_3\left(\frac{\theta_D}{T}\right) = \frac{C_v}{NR} = \left(\frac{12\,T^3}{\theta_3^3}\right)\int_0^{\theta_3/T} \frac{x^3 dx}{\exp(x-1)} - \frac{3\theta_D/T}{\exp(\theta_D/T)-1} \tag{2}$$

For two- or one-dimensional structures, such as are found in crystals of layer and chain molecules, the frequency distribution changes to linear and constant functions, respectively. The corresponding integrals are called the two- and one-dimensional Debye functions (60,61)

$$D_2\left(\frac{\theta_2}{T}\right) = \frac{C_v}{NR} = \left(\frac{6T^2}{\theta_2^2}\right)\int_0^{\theta_2/T} \frac{x^2 dx}{\exp(x)-1} - \frac{2\theta_2/T}{\exp(\theta_2/T)-1} \tag{3}$$

$$D_1\left(\frac{\theta_1}{T}\right) = \frac{C_v}{NR} = \left(\frac{2T}{\theta_1}\right)\int_0^{\theta_1/T} \frac{x\,dx}{\exp(x)-1} - \frac{\theta_1/T}{\exp(\theta_1/T)-1} \tag{4}$$

The N in equations 1-4 refers to the appropriate number of vibrators and x stands for $h\nu/kT = \theta/T$. The sum of all N is three times the number of atoms in a repeating unit, the number of degrees of freedom. Tarasov proposed a special combination of equations 2 and 4 for the skeletal vibrations of a linear chain (62)

$$T(\theta_3/T,\ \theta_1/T) = \frac{C_v}{NR} = D_1(\theta_1/T) - (\theta_3/\theta_1)\left[D_1\left(\frac{\theta_3}{T}\right) - D_3\left(\frac{\theta_3}{T}\right)\right] \tag{5}$$

Table 2. Group Vibration Frequencies of Polytetrafluoroethylene

	Einstein terms		Box distribution		
Normal mode	N_E	ν_E (cm^{-1})	N_b	ν_L (cm^{-1})	ν_U (cm^{-1})
ν_1 (asymmetric CF_2 stretching)	0.20	1449	0.67	1250	1440
	0.13	1256			
ν_2 (C—C stretching)			0.53	1161	1379
			0.47	1161	1229
ν_3 (symmetric CF_2 stretching)	0.17	1149	0.83	723	1154
ν_4 (CF_2 wagging)	0.20	576	0.20	630	672
			0.60	587	672
ν_5 (CF_2 rocking)	0.27	755	0.73	307	519
ν_6 (CF_2 bending)	0.13	385	0.87	283	385
ν_7 (CF_2 twisting)	0.23	294	0.77	190	289

The Tarasov equation holds for most linear macromolecules. Its limits are reached when phenylene groups are included in the backbone chain as in poly(oxy-1,4-phenylene) or poly(ethylene terephthalate) (63), or alternating heavy and light mass backbone units occur, as in poly(vinylidene fluoride) or poly(vinylidene chloride)s (64). A detailed analysis of skeletal vibration is available (32). Table 1 lists data of N, θ_1 and θ_3 for a selected number of polymers. For group vibrations, which are usually of much narrower distribution, it is sufficient to use single-frequency Einstein terms or to average over a frequency range that leads to a box-distribution function

$$B\left(\frac{\theta_U}{T}, \frac{\theta_L}{T}\right) = \frac{C_v}{NR} = \frac{\theta_U}{(\theta_U - \theta_L)}\left[D_1\left(\frac{\theta_U}{T}\right) - \frac{\theta_L}{\theta_U} D_1\left(\frac{\theta_L}{T}\right)\right] \tag{6}$$

where θ_U and θ_L are the upper and lower frequencies of the group vibrational range. Table 2 shows, as an example, the various approximated frequency regions used for the group-vibration spectrum of polytetrafluoroethylene as derived from a dispersion curve.

In the final step of computation, C_v is connected with the measured C_p. Both the thermal expansivity α and the isothermal compressibility κ must be known for this thermodynamics-based calculation

$$C_p - C_v = \alpha^2 VT/\kappa \tag{7}$$

where V represents the molar volume. Since α and κ are usually, at best, available at one temperature, the semiempirical Nernst–Lindemann expression must be utilized with modifications that account for the slow excitation of the vibrations involving the light atoms and strongly bound atoms in polymers (65,66)

$$C_p - C_v = 3RA_0 C_p T / T_m^0 \tag{8}$$

where $T_m{}^0$ is the equilibrium melting temperature and A_0 is a constant that for many polymers has a value close to 3.9×10^{-3} K · mol/J (66).

In the temperature region from above 100 K to the glass or melting transition, the intramolecular skeletal vibrations of most polymers can be evaluated after computation of the group vibrations. The intermolecular vibrations are commonly already excited at 100 K, while the remaining skeletal vibrations approach full excitation at room temperature, and then contribute a constant amount NR to the heat capacity. The values of the skeletal vibrations, N, are listed in Table 1, together with the temperature range of available experimental data. The group vibrations, as listed in Table 2 for polytetrafluoroethylene, cause another gradual increase in C_p above room temperature (note that the repeating unit is CF_2- and not C_2F_4-). It can be seen in Figure 2 that the Dulong–Petit high temperature limit for the heat capacity at constant volume, C_v, for polyoxymethylene of $12\,R = 100$ J/(K · mol) is not reached at the decomposition temperature. The highest frequencies are the CH_2 stretching vibration (as high as 4000 K).

Between the glass and melting transitions of semicrystalline macromolecules, special thermal effects can be observed. Semicrystalline macromolecules have a microphase- or nanophase-separated structure with many molecules bridging two or more phases in a nonequilibrium state. As soon as the noncrystalline portions of the molecules experience a glass transition, C_p increases. The phase boundaries result in a broadening of the glass-transition region of partially crystalline polymers beyond the high temperature end seen in noncrystalline samples due to stress transmitted into the noncrystalline phase. A detailed thermal analysis of poly(ethylene terephthalate) showed drastic changes of the relaxation energies on partial crystallization (see also Figure 11, below) (67,68). Often the increase in C_p is, in addition, less than expected from the crystallinity determined from the heat of fusion when assuming a macroscopic two-phase system (crystallinity model). The missing increase in C_p was proposed to be caused by a third phase, a rigid–amorphous nanophase, as part of the semicrystalline structure (69). In the meantime, TMDSC allowed to demonstrate that the rigid–amorphous phase RAF is produced at the same time as the crystals, and also disappears along with the crystals and may show a separate T_g below or above the melting temperature (8). In the second case, melting is retarded because of a limited mobility in the rigid noncrystalline phase (70).

Increases as well as decreases in enthalpy can also be observed between T_g and T_m in case the phase-structure changes, ie, the composition changes because of a latent heat. The change of the enthalpy is then not only caused by a heat capacity, $(\partial H/\partial T)_{n,p}$, but must be written as

$$dH = (\partial H/\partial T)_{n,p}\, dT + (\partial H/\partial T)_{T,p}\, dn \tag{9}$$

or, if the crystallinity w^c changes in a measurable way with temperature, as

$$dH/dT = C_p^{\#} = w^c C_{p,c} + (1 - w^c) C_{p,a} - \Delta H_f (dw^c/dT) \tag{10}$$

Treating dH/dT as an "apparent" heat capacity $C_p{}^{\#}$, equation 10 allows the separation of the latent heat contribution from the thermodynamic heat capacity if $C_{p,c}$ and $C_{p,a}$, the crystalline and amorphous heat capacities, are known (as well as the temperature-dependence of the heat of fusion, ΔH_f).

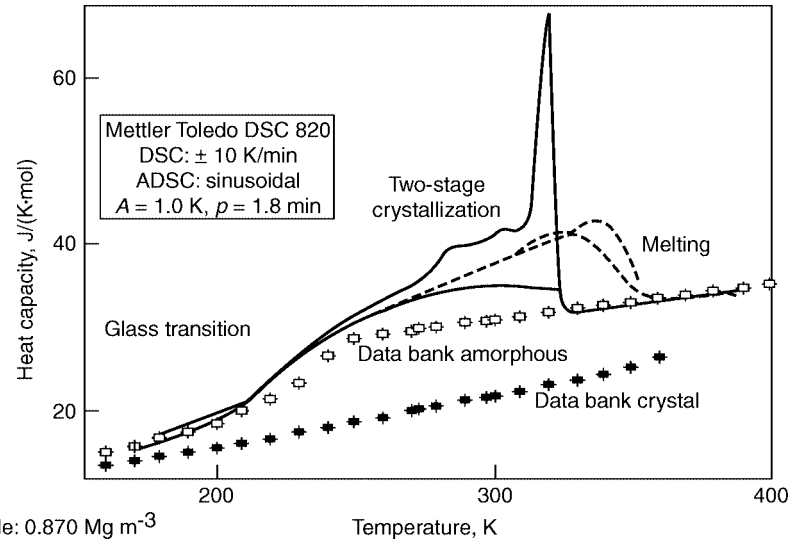

Fig. 3. Differential thermal analysis of linear low density polyethylene on cooling (continuous lines), followed by heating (broken lines), showing a high content of reversing crystallization and melting. Standard DSC: thin lines; TMDSC: thick lines. The overall supercooling contrasts the partially reversible crystallization and melting after an overall metastable, semicrystalline structure has been set up on the initial cooling. The modulation amplitude on TMDSC is given by the letter A, and the modulation period by p.

Well-known processes which can decrease or increase the enthalpy of a nonequilibrium, semicrystalline polymer on its path to higher stability are premelting (11), crystal perfection, reorganization, recrystallization (9,10), and cold crystallization (71). Recently it was found that within the metastable, global nanophase structure of semicrystalline polymers, it is also possible to observe local, reversible phase equilibria (8). Special techniques of the temperature-modulated DSC must be used to get quantitative information about the reversible equilibria. Folded-chain crystals and fringed-micellar structures show considerable reversibility in the crystallization and melting range. Figure 3 compares, as an example, TMDSC cooling and heating curves with analogous, standard DSC traces for linear low density polyethylene. The high temperature crystallization and melting mainly represents chain-folded crystals with partial reversibility. Closer toward T_g, fringed micellar crystals prevail with almost complete reversibility. More rigid macromolecules, as well as extended-chain molecules, do not exhibit such reversibility, as is shown in Figure 4, for extended-chain polyethylene (8).

The heat capacity of liquid macromolecules can be measured above the glass-transition or the melting-transition temperature. The group vibrations change little on fusion. The changes of the skeletal vibrations due to volume expansion also have little influence on heat capacity, since, once excited, the heat capacity contribution remains unchanged on lowering of the frequency. The change in volume expansion is noticed in a sizable increase in C_p at the glass transition, caused largely by a potential energy increase (hole formation). However,

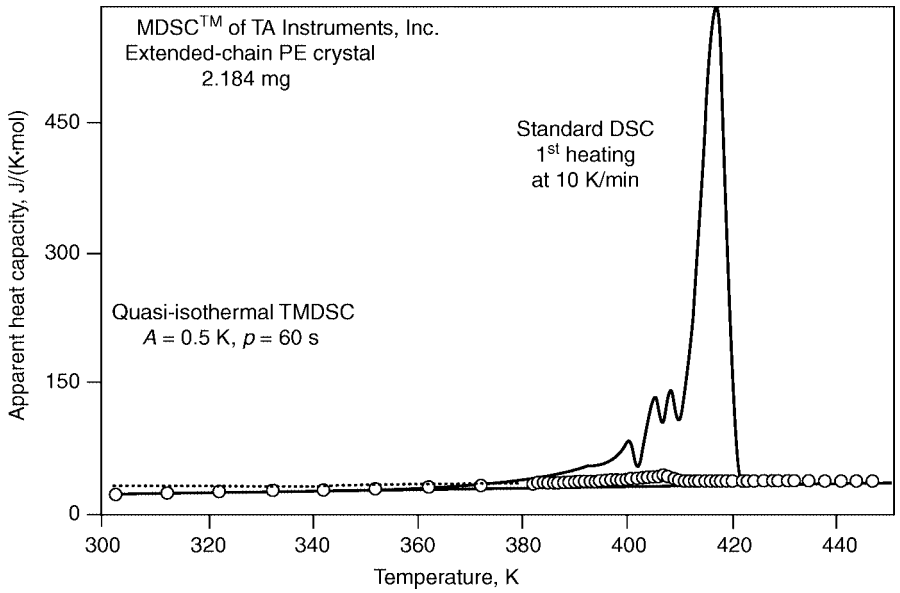

Fig. 4. Analysis of the melting of extended-chain crystals of polyethylene grown to 98% crystallinity, using high pressure crystallization (9,10,13). The standard DSC shows the sum of the latent heat and heat-capacity contributions of equations 9 and 10. The minor low temperature peaks reveal low molecular mass fractions and a small amount of remaining chain folding. The quasi-isothermal TMDSC was carried out sequentially for 20 min or longer at the temperatures indicated by the small circles. ○ 1st heating. The modulation had an amplitude A and period p. Practically no reversing melting can be seen. The small remaining reversible fraction could be accounted for quantitatively by the low molar mass portion and the remaining chain folding (8).

quantitatively, little is known about the theory of liquid heat capacity. Attempts to compute heat capacities of liquid macromolecules were based on a separation of the partition function into a vibrational part (approximated by the vibrational spectrum of the solid, as described above), a conformational part [approximated by the rotational isomers model (72) or a description using a one-dimensional Ising model (73)], and an external, configurational part (approximated by data derived from the difference in heat capacity at constant pressure and volume as given by eq. 7).

Empirically, liquid heat capacities are often observed to change linearly with temperature. They have a smaller increase with temperature than solids, and are additive with regard to their constituent groups. In case of atomic backbone repeating units, such as Se (74), O (75), or S (76), the group contribution of the heat capacity decreases with temperature. This occurs most likely because of increasing changes of vibrational modes of motion to internal rotations whose heat capacity contributions decrease with temperature from R to $R/2$. Table 3 shows the relationship between C_p and temperature T for common groups, based on an empirical addition scheme (77). An error of less than $\pm 5\%$ in the temperature range of 250–750 K is typical. References to all known liquid heat capacities and their temperature ranges are given in Table 1.

Table 3. Relationships between Liquid C_p and Temperature T for Different Structure Groups in Linear Macromolecules

Group	$C_{p,\mathrm{a}}$, J/(K · mol)
Methylene, CH_2	$0.0433\,T + 17.92$
Phenylene, C_6H_4	$0.1460\,T + 73.13$
Carboxyl, COO	$0.002441\,T + 64.32$
Carbonate, OCOO	$0.06446\,T + 84.54$
Dimethylmethylene, $C(CH_3)$	$0.2013\,T + 18.79$
Carbonyl, CO	$0.07119\,T + 32.73$
Naphthylene, C_6H_{10}	$0.2527\,T + 114.49$
Dimethylphenylene, $C_6H_2(CH_3)_2$	$0.2378\,T + 111.41$
Oxygen, O	$-0.00711\,T + 28.13$
Sulfur, S	$-0.02028\,T + 46.59$
Selenium, Se	$0.000032608\,T^2 - 0.049766\,T + 52.408$

Other Thermodynamic Functions

Enthalpy, Entropy, and Free Enthalpy. By knowing solid and liquid heat capacities of linear macromolecules, other thermodynamic functions can be obtained through the following relationships

$$H_\mathrm{T} - H_0 = \int_0^T C_p \, \mathrm{d}T \tag{11}$$

$$S_\mathrm{T} - S_0 = \int_0^T \frac{C_p}{T} \, \mathrm{d}T \tag{12}$$

$$G_\mathrm{T} = H_\mathrm{T} - TS_\mathrm{T} \tag{13}$$

For perfect, crystalline solids, the entropy at 0 K is zero, ${S_\mathrm{c}}^0 = 0$. Thus, absolute entropies can be calculated directly. Information to the available data is given in Table 1. For crystalline, linear macromolecules, the derived thermodynamic functions are reported as follows

$$\begin{array}{rc} \textit{Enthalpy}: & H^c_\mathrm{T} - H^c_0 \\ \textit{Entropy}: & S^c_\mathrm{T} \\ \textit{Free enthalpy}: & G^\mathrm{c}_\mathrm{T} - H^c_0 \end{array}$$

For amorphous solids, the residual entropy at 0 K can be calculated by equating the entropy at the equilibrium melting temperature ${T_\mathrm{m}}^0$

$$S^c_{T^0_\mathrm{m}} + \Delta S_\mathrm{f} = S^a_{T^0_\mathrm{m}} \tag{14}$$

where ΔS_f is the equilibrium entropy of fusion of fully crystalline solids. It follows that

$$S^\mathrm{a}_0 = S^\mathrm{c}_{T^0_\mathrm{m}} + \Delta S_f - \left(S^\mathrm{a}_{T^0_\mathrm{m}} - S^\mathrm{a}_0\right) = \int_0^{T^0_\mathrm{m}} \left(C^\mathrm{c}_p - C^\mathrm{a}_p\right) d(\ln T) + \Delta S_f \tag{15}$$

An analysis of many macromolecules indicates that the residual entropy of amorphous macromolecules at absolute zero is 2–4 J/K · mol per mobile bead, as listed in Table 1 (76,77). With the knowledge of $S_0{}^a$, the absolute entropy of amorphous solids can be calculated. The crystalline state at 0 K is chosen as a standard state for all enthalpy and free enthalpy data. The functions $(H_T{}^a - H_0{}^c)$ and $H_T{}^c - H_0{}^c)$ are directly related to the heats of fusion at temperature T

$$H_T^a - H_0^c = \left(H_T^a - H_0^a\right) + \left(H_0^a - H_0^c\right) \tag{16}$$

$$H_0^a - H_0^c = \left(H_{T_m^0}^c - H_0^c\right) + \Delta H_f - \left(H_{T_m^0}^a - H_0^a\right) \tag{17}$$

From the absolute entropy and $H_T{}^a - H_0{}^c$, the free enthalpy (Gibbs function) $G_T{}^a - H_0{}^c$ can be calculated for amorphous solids. For amorphous linear macromolecules, the reported thermodynamic functions listed in the sources for Table 1 are

Enthalpy:	$H_T^a - H_0^a$, $H_T^a - H_0^c$
Entropy:	$S_T^a - S_0^a$, S_T^a
Free enthalpy:	$G_T^a - H_0^c$

Figure 5 shows the changes of these thermodynamic functions of polyethylene with temperature.

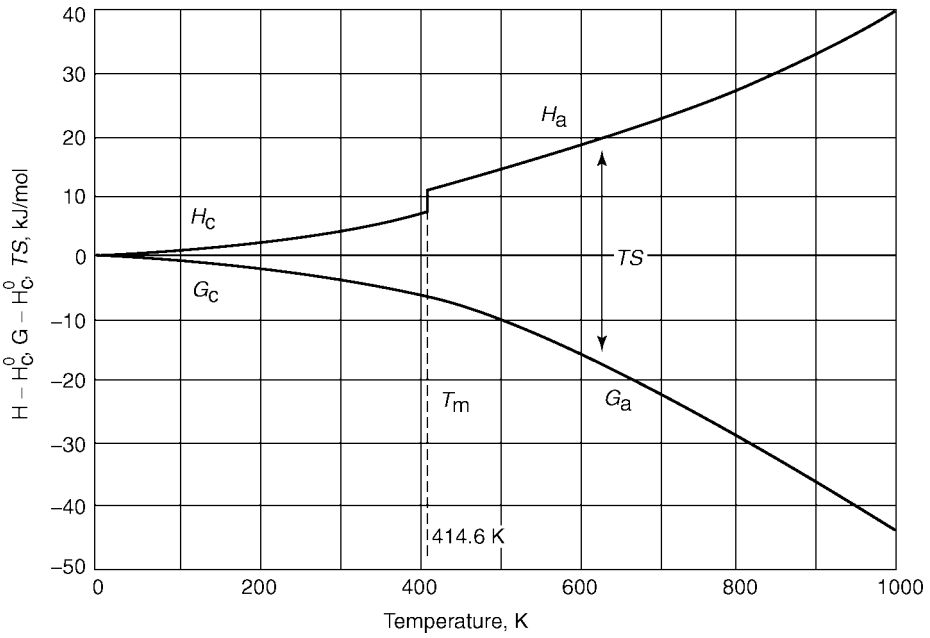

Fig. 5. Enthalpy, entropy, and free enthalpy of polyethylene as derived from heat capacities. The origin of H and G has been set arbitrarily to zero at absolute zero in temperature, and the energy equivalent TS is plotted instead of S.

Table 4. Pressure–Volume–Temperature Data of Macromolecules[a]

Polymer	Temperature range, K	Pressure, Pa $\times 10^4$	Ref.
Polyethylene, linear	414–472	0–2000	80
Polyethylene, branched	385–498	0–2000	81
Isotactic polypropylene	443–570	0–2000	82
Isotactic poly(1-butene)	406–519	0–2000	82
Poly(4-methyl-1-pentene)	508–615	0–2000	83
Polytetrafluoroethylene	603–645	0–400	84
Poly(ethylene terephthalate)	543–615	0–2000	85
Polysulfone	468–643	0–2000	86
Polystyrene	223–523	100–1800	87
Polycarbonate	303–613	100–1800	86
Polyarylate	303–613	100–1800	86
Phenoxy resin	303–573	100–1800	86

[a] To convert Pa to mm Hg, multiply with 0.0075.

Pressure, Volume, and Temperature. The pressure–volume–temperature (PVT) diagrams of linear macromolecules in different states provide another set of important thermodynamic functions, as is shown in Figure 6, for polypropylene. Using high pressure dilatometry, macromolecules have been analyzed in their liquid states, as shown in Table 4. All data can be fitted to the empirical Tait equation listed in Figure 6. Both constants of the Tait equation are exponential functions of temperature.

Empirical Tait equation: $v(p,T) = v_0(T)\{1 - 0.0894 \ln[1 + p/B(T)]\}$

$v_0(T) =$ Volume at zero (atm) pressure

$B(t) =$ Tait parameter

Theoretical treatments of the equation of state are based on the lattice theory. The Simha–Somcynsky theory suggests a hole theory of polymeric liquids by determination of the reduced parameters p^*, v^*, and T^* (78,79). This statistical

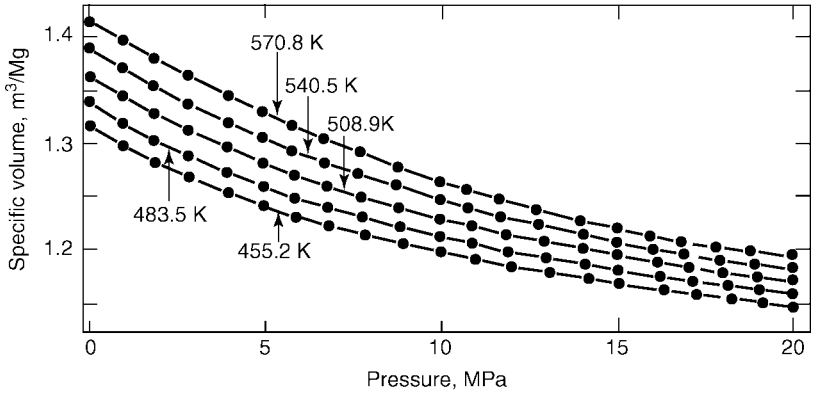

Fig. 6. Experimental (circles) and theoretical (curves) isotherms for polypropylene. The curves are based on the Simha–Somcynsky theory and show good agreement with the data ($v^* = 1.1954$ cm^3/g, $p^* = 530$ kPa, $T^* = 11{,}155$ K) (78,79).

mechanical theory describes a polymer melt as consisting of N molecules having s segments, each of which need not be identical to the chemical repeating unit. They are placed in a quasi-lattice of coordination number z, with the fraction y of the lattice sites occupied; the hole fraction is, thus, $1 - y$. Each molecule is to have $3c$ external (volume-dependent) degrees of freedom. A "square-well" approximation of the 6–12 potential is used as intersegmental potential, specified by the potential energy minimum ε^* and the hardcore volume v^* of the segment. The partitionfunction of the system contains a Boltzmann lattice–energy factor, a combinatorial factor representing the entropy of segment mixing and empty lattice sites, and a statistical-mechanical free-volume term. From the partition function, the equation of state may be calculated in the form of

$$\tilde{p}\tilde{v}/\tilde{T} = f[\tilde{v},\ \tilde{T},\ y(\tilde{v},\ \tilde{T})] \tag{18}$$

The function $y(\tilde{v},\ \tilde{T})$ is determined by the minimization of the Helmholtz free energy with respect to y.

$$(\partial \tilde{F}/\partial y)_{\tilde{v},T} = 0 \tag{19}$$

This leads to a transcendental equation for y which requires numerical solution. The equation of state and the determining equation for y are written in terms of reduced variables $\tilde{p} = p/p^*$, $\tilde{v} = v/v^*$, and $\tilde{T} = T/T^*$. The reducing parameters, p^*, v^*, and $T,^*$ contain the molecular characteristics of the system as follows (for a system of one gram of material) (88,89)

$$v^* = Nsu^* = (N_A/M)v^* \tag{20}$$

$$T^* = (z-2)s\epsilon^*/ck \tag{21}$$

$$p^* = (z-2)\epsilon^*/v^* \tag{22}$$

where N_A represents Avogadro's number, M is the molecular mass per segment, and k is the Boltzmann constant. Even though the equation of state is written in terms of reduced variables, it does not conform to a principle of corresponding states since the determining equation of y also explicitly contains the flexibility ratio $3c/s$. However, the equations of state calculated for different values of $3c/s$ are superimposable. This means that the equation of state effectively conforms to a principle of corresponding states, but it also means that the ratio $3c/s$ cannot be calculated from PVT data. Conventionally, the theoretical equation of state is evaluated by setting $3c/s = 1$ ie, the theory is formulated in terms of an effective segment having exactly one external degree of freedom. The molecular mass M_0 of this segment follows to be

$$p^*v^*/T^* = (1/3)kN_A/M_0 = R/3M_0 \tag{23}$$

where R is the gas constant. The choice $3c/s = 1$ makes T^* directly proportional to the energy parameter of the effective segment, and $M_0v^* = N_Av^*$ becomes the molar hardcore volume of the effective segment.

In order to avoid the uncertainty of the parameter c which characterizes the decrease in the external degrees of freedom, a much simpler mathematical form of the equation of state was proposed on the basis of the Ising (lattice) fluid model (88,89)

$$\tilde{\rho}^2 + \tilde{p} + \tilde{T}[\ln(1-\tilde{\rho}) + (1-1/r)\tilde{\rho}] = 0 \tag{24}$$

where $\tilde{\rho}$ is the reduced density ($\tilde{\rho} = \rho/\rho^*$), $\tilde{p}$ and $\tilde{T}$ are the same as defined above, and r is the number of lattice sites occupied by the r-mer. These equation-of-state parameters are related to the molecular mass M by

$$RT^* \ \rho^*/p^* = M/r \tag{25}$$

where R is again the gas constant.

Since r remains explicit in the reduced equation of state, a simple corresponding-state principle is not, in general, satisfied. For a polymeric liquid, however, $r \to \infty$, and the equation of state is reduced to

$$\tilde{\rho}^2 + \tilde{p} + \tilde{T}[\ln(1-\tilde{\rho}) + \tilde{\rho}] = 0 \tag{26}$$

Thus, all polymer liquids of sufficiently high molecular mass should satisfy a corresponding-state principle.

Earlier than either of the two theories mentioned above, Flory and co-workers (90,91) proposed an equation of state in a reduced form as

$$\tilde{p}\tilde{v}/\tilde{T} = \tilde{v}^{1/3}/(\tilde{v}^{1/3} - 1) - (1/\tilde{v}\tilde{T}) \tag{27}$$

Again, the reduced variables are defined as they were before: $\tilde{p} = p/p^*$, $\tilde{v} = v/v^*$, and $\tilde{T} = T/T^*$. In this theory, the reduced quantities (with an asterisk) reflect the molecular characteristics of the system.

Experimental PVT data reported so far have been described best by using the Simha-Somcynsky equation (eq. 18) (78,79), and somewhat less well by equation 27 (90,91). Equation 24 (88,89) is substantially poorer, especially at elevated pressure.

All PVT diagrams studied so far refer to polymer liquids. Substantial experimental difficulty arises in the extension to the semicrystalline state because of the nonequilibrium nature. No determined attempt at extrapolation to equilibrium data has been made to date, despite the possibility to approximate equilibrium crystal properties from unit cell parameters of X-ray data.

Transition Properties

First-Order Transitions. The principal transitions in macromolecules are those concerned with enthalpy (latent heat) and entropy changes. They are called first-order transitions according to a classification requiring the first derivative of the change in free enthalpy with respect to temperature not to be zero (92). For a single-component system (pure compound), thermodynamic equilibrium states

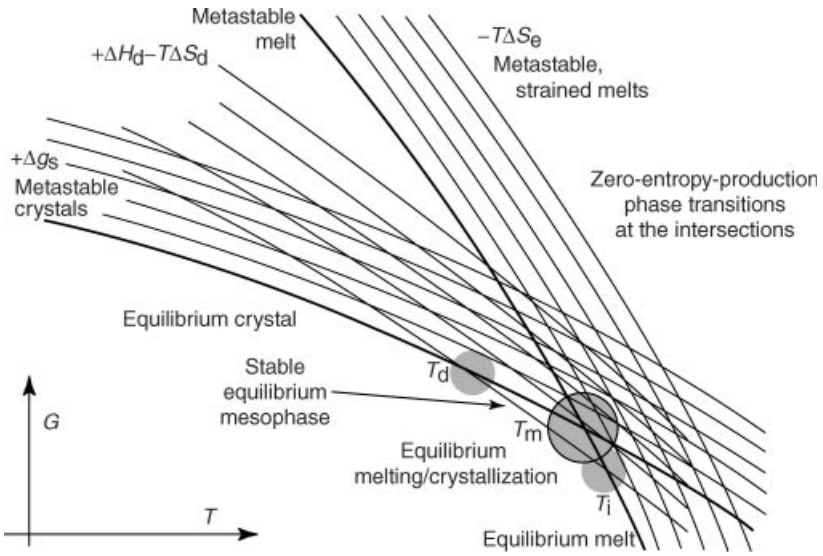

Fig. 7. Free enthalpy of equilibrium and metastable states. The solid lines represent G of the equilibrium crystal and liquid and their extrapolations beyond T_m. The G of metastable crystals and melts are largely parallel to the equilibrium states. Adding a mesophase with an intermediate entropy between liquid and solid may produce, as shown, an equilibrium mesophase between T_d, of disordering and T_i, the temperature of isotropization. Such mesophase shifts T_m into the nonequilibrium region.

are always at the lowest Gibbs energy G, as shown in Figure 7. A crystal must melt at a sharp melting temperature $T_m{}^0$. The transition shows a change in the slope of free enthalpy in going from one phase to the other. The relationship of the melting temperature to changes in enthalpy and entropy is

$$T_m^0 = \frac{\Delta H_f^0}{\Delta S_f^0} \tag{28}$$

where $\Delta H_f{}^0$ and $\Delta S_f{}^0$ are the heat and entropy of fusion, respectively.

Equilibrium crystals are defined as crystals with negligible surface effects (of infinite size) and, if any, only equilibrium defects. Complications exist, however, in the study of the transition of linear macromolecules caused by a common formation of lamellar or fibrillar crystals which are metastable and contain nonequilibrium defects (9). Therefore, even pure, one-component, crystalline macromolecules have usually a broad melting-transition range and do not approach equilibrium, although it was found recently that local equilibria may exist on the overall metastable phase structure (8). The experimental methods to approach equilibrium developed for nonpolymeric materials involving slow heating or annealing before analysis were singularly unsuccessful for macromolecules (11).

Early observations of melting transitions revealed the change of three thermodynamic functions, the degree of order (entropy), volume, and enthalpy. For the first function, a general statement about the different contributions from

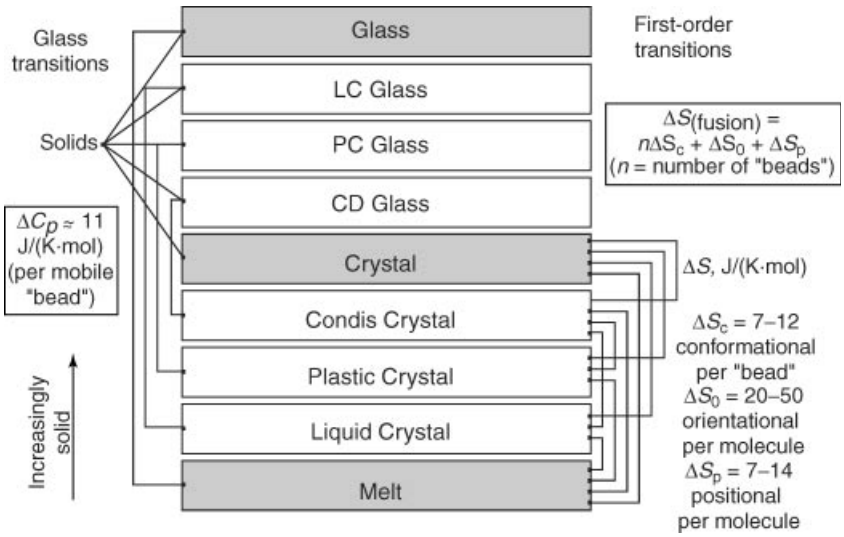

Fig. 8. Illustration of the classical condensed phases (melt, crystal and glass) and the six possible mesophases (liquid, plastic, and condis crystals and their corresponding glasses). The possible first-order transitions and their entropies of transition are marked on the right and the glass transitions and their change in heat capacity at T_g, on the left.

positional, orientational, and conformational entropy changes can be made (11). In fact, a general scheme of these entropy contributions was developed (12), as is shown in Figure 8. The most important mesophases for macromolecules are the liquid and condis crystals (13).

No such statement can be made for the volume or enthalpy changes on transition, although similar crystal structures and molecules may lead to similar changes (93). Further general observations on fusion are the lowering of ${T_m}^0$ by solvents (as a second, noncrystallizable component) and the lowering of ${T_m}^0$ for small crystals (11). The last effect has also been used to describe the fusion of small, nonequilibrium crystals as commonly found in metastable, semicrystalline polymers (11,94).

To find the equilibrium melting temperature and heat of fusion, extrapolations must be made from measurements on metastable, small crystals or on equilibrium crystals of small molecules. Only since the 1960s are crystals of extended chain macroconformation and macroscopic size available for some macromolecules. These crystals have been analyzed with respect to their melting behavior (11,95,96), which permits the discussion of equilibrium melting from both an experimental and a theoretical point of view. Although these equilibrium crystals cannot grow at ${T_m}^0$, their melting can be observed at ${T_m}^0$. Table 1 also gives a summary of all critically reviewed heats of fusion and equilibrium melting temperatures. These data deviate substantially from those expected from nonequilibrium experiments (11).

In addition to complete, one-step fusion, it is possible that some order is retained during a phase transition of the first order. In this case, mesophases are formed as shown in Figure 8. These are phases of intermediate order and mobility

(12). The entropy of fusion may be approximated by

$$\Delta S_f = \Delta S_{pos} + \Delta S_{or} T + n \Delta S_{conf} \quad (29)$$

where the three ΔS contributions are due to positional, orientational, and conformational entropy changes during the transitions. Only the last term depends on molecular size n, as also shown in Figure 8. The liquid crystals retain a small amount of orientational order because of the presence of a rod-or disk-like mesogen in the molecule; plastic crystals retain full positional order because of an almost spherical molecular shape, which permits rotation in the crystal; and condis crystals show dynamic conformational disorder in the crystal.

The phase changes of semicrystalline macromolecules that are usually not in equilibrium must make use of irreversible thermodynamics (11,97). On the other hand, even a system that is initially in equilibrium may go through a nonequilibrium transition because of kinetic restrictions, such as the superheating of crystals (98) or the more widely recognized supercooling of polymer melts on crystallization (10). The latter cases are often treated by kinetic arguments by introducing nucleation barriers (10,88,89,99).

Trying to obtain data from nonequilibrium experiments, one finds that the metastability of the system can change during the study. In order to avoid or distinguish those effects, three methods have been developed and are commonly applied for the study of nonequilibrium phase transition. The first involves the study of the transition as a function of time; the second avoids changes in the amorphous–crystalline interface by cross-linking the molecules; and the third hinders reorganization through chemical etching of the amorphous areas, producing small, equilibrium (but oligomeric) crystals, the transitions of which can be related to the small polymer crystals (11). Equilibrium transitions to be compared to the nonequilibrium measurements are listed in Table 1.

Glass Transitions. The glass-transition temperature is the main characteristic of the solid and mobile states of macromolecules with mesophase or amorphous structure. The mobile states become solid on cooling through the glass-transition temperature if crystallization does not intervene, as indicated in Figure 8. The microscopic process involved is the freezing of large-scale, molecular motion without change in structure. Since the heat capacity of the glass is always lower than that of the liquid at the same temperature, and since there is no latent heat involved, the glass transition takes superficially the appearance of a thermodynamic second-order transition (92). The freezing of molecular motion is, however, time-dependent, and, therefore, the glass transition must be called an irreversible process, and its characterization must include the time scale of the measurement. The glass transition occurs at a recognizable transition temperature because of a rather large temperature dependence of the relaxation time for large-scale molecular motion (micro-Brownian motion). Since the glass transition occurs over a larger temperature region, a characterization must involve five temperatures, as shown in Figure 9. The glass-transition temperature T_g is commonly the temperature of half-freezing, as it can be determined by heat capacity, expansion coefficient, or compressibility, as examples.

Detailed, and sometimes conflicting, theories of the glass transition, mainly applied to linear macromolecules, are discussed elsewhere (100–107). The theories

are all simplified and do not describe the glass transition fully. Their principal shortcoming is the omission of the cooperative nature of the glass transition. Unfreezing one configuration significantly helps the neighboring molecular segments to move. The frequency dependence of the glass transition cannot only be determined by mechanical analysis and dielectric measurements, but also with temperature-modulated calorimetry. A comparison of the different results is available (108,109) (see, GLASS TRANSITION).

A critical survey of over 20 macromolecules revealed that the heat capacity increase at the glass-transition temperature is about 11.3 J/K per mole of mobile units (110). The division of a repeating unit into mobile units is not fully unambiguous. However, independent motion can be expected between the different rotational isomers for mobile groups as, for example, for phenylene, carboxyl, or methylene groups. These groups are then to be counted as separate mobile units. Furthermore, the effect of a mobile unit is somewhat size-dependent. Large units seem to contribute two times or even three times the increase in heat capacity at the glass transition (76,77,111). In Table 1, the number of mobile units, assumed for the respective repeating units, is given in parentheses in column 2. Also listed are critically reviewed glass-transition temperatures and heat capacity increases at the glass-transition temperature.

The change in volume V, enthalpy H, and entropy S, as well as the derivative heat capacity C_p, and thermal expansivity α on cooling and heating are shown schematically in Figure 10. Coupling equal heating and cooling rates leads to the glass-transition behavior which is illustrated in Figure 9. It permits measurement on heating as well as on cooling. The thermodynamic quantities change almost reversibly between the values characteristic for the glass and the liquid at a temperature determined by the time scale of measurement. Different cooling and heating rates cause hysteresis effects. Shown is an endotherm after the glass transition due to slower cooling than heating.

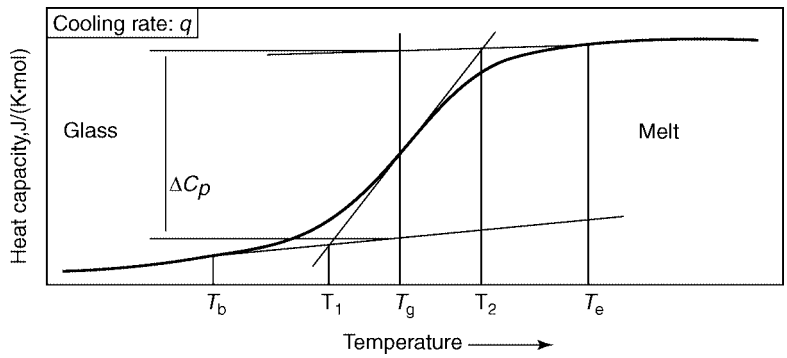

Fig. 9. Heat capacity in the glass-transition region. The first perceptible beginning of the glass transition T_b is judged by the first increase in C_p from that of the solid state; T_1 and T_2 are the extrapolated beginning and end of the glass transition. The difference between T_1 and T_2 is indicative of the broadness of the main portion of the glass transition. The glass-transition temperature T_g is chosen at half-devitrification when judged by the C_p increase. The temperature T_e is the end of glass transition; it is reached when C_p attains the value of the mobile phase. The time-scale is fixed by the cooling rate q.

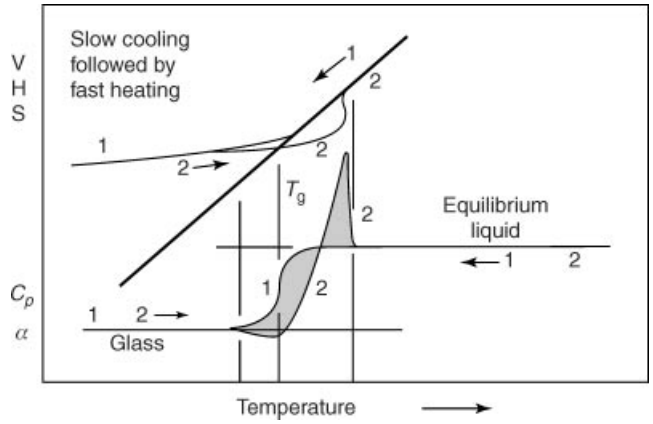

Fig. 10. Schematic drawing of the changes in volume, enthalpy, entropy, and the derivative properties (heat capacity C_p and expansivity α) on slow cooling followed by fast heating through the glass-transition region. The numeral 1 marks the response on cooling, the numeral 2, on heating. The two shaded areas are of equal magnitude and can be used to characterize the thermal history.

The glass transitions are not only affected by their previous thermal history, as demonstrated in Figure 10, but also by their mechanical (and dielectric) history. Stress, induced during sample processing such as drawing, may be frozen in on cooling through T_g. The stress introduces weak points with respect to chemical degradation. On heating into the vicinity of the glass transition, the stress causes shrinkage or deformation of the sample. Thermal analysis can detect the stress as it is released at T_g in the form of an exotherm. While exotherms induced by hysteresis decrease with increasing heating rate when a quickly cooled sample is reheated more slowly and may even turn into endotherms, the stress-related exotherms are of constant area (enthalpy) and may only broaden over a wider temperature range with increasing heating rate.

Semicrystalline samples show changes in the glass transition of the amorphous fraction which lead to a broadening of the transition range and shifts of the midpoint of the transition to higher temperature. In addition, the crystals may form a rigid–amorphous fraction, as described in the section about the heat capacities of solids and liquids at the beginning of this article on thermodynamic properties (75–77). Figure 11 illustrates the change of the glass transition of amorphous poly(ethylene terephthalate) with increasing crystallinity. The absolute levels of the heat capacity after the glass transition do not correspond to the level of crystallinity. The missing increase in heat capacity is linked to the presence of a rigid–amorphous fraction which undergoes its glass transition at a higher temperature (67), as was described above, in connection with the discussion of the heat capacity of semicrystalline structures.

Liquid Multicomponent Systems. For the description of multicomponent systems, the number of moles, N_i, or concentrations of each of the components is added to temperature and pressure as variables of state. For each extensive function of state, such as *V, U* (internal energy), *S, G, H*, C_p, and C_v (for example,

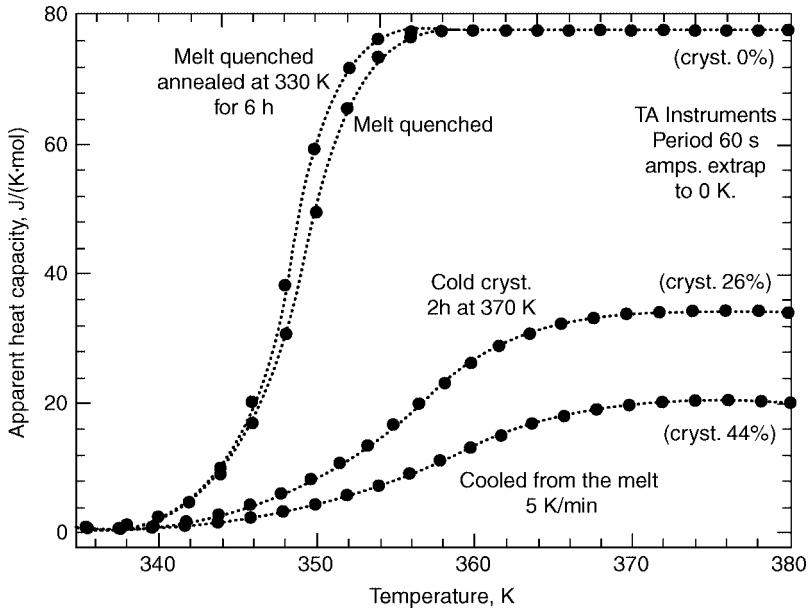

Fig. 11. Glass transitions of poly(ethylene terephthalate) with different degrees of crystallinity produced by the indicated thermal histories. The curves were measured with quasi-isothermal TMDSC at the temperatures marked by the filled circles, with modulation amplitudes extrapolated to zero and periods of 60 s (67).

for each component A, B, etc), the following derivatives can be written

$$\left(\frac{\partial X}{\partial N_{\mathrm{A}}}\right)_{T,p,N_{\mathrm{B}}} = X_{\mathrm{A}}, \left(\frac{\partial X}{\partial N_{\mathrm{B}}}\right)_{T,p,N_{\mathrm{A}}} = X_{\mathrm{B}} \tag{30}$$

The quantities X_{A}, X_{B}, etc, are called the partial molar quantities. The partial molar free enthalpy is also called the chemical potential and given the letter μ. In general, the partial molar quantities are not additive, but the following relationship can be derived between two different components (easily generalized for multicomponent systems)

$$dX = X_{\mathrm{A}}\, dN_{\mathrm{A}} + X_{\mathrm{B}}\, dN_{\mathrm{B}} \tag{31}$$

Integration of equation 29 without changing the composition gives

$$X = N_{\mathrm{A}}X_{\mathrm{A}} + N_{\mathrm{B}}X_{\mathrm{B}} \tag{32}$$

The total differential of equation 31 must be

$$dX = X_{\mathrm{A}}\, dN_{\mathrm{A}} + N_{\mathrm{A}}\, dX_{\mathrm{A}} + X_{\mathrm{B}}\, dN_{\mathrm{B}} + N_{\mathrm{B}}\, dX_{\mathrm{B}} \tag{33}$$

Comparison of the coefficients of equations 32 and 30 reveals the important equations

$$N_A\, dX_A + N_B\, dX_B = 0 \text{ or } dX_A = -\left(\frac{N_B}{N_A}\right) dX_B \tag{34}$$

which permit the calculation of the change in partial molar quantities of one component from the other.

Whether a single-phase solution or several phases are formed in a multicomponent system depends on compatibilities among the components. Generally speaking, three kinds of compatible systems are possible when dealing with macromolecules. Best known are the cases 1 and 2 which concern compatibility of small molecules with macromolecules and one macromolecule with another. The special effect introduced by the macromolecule is caused by its large molecular size, as expressed by the Flory–Huggins equations, given, below. The third kind involves the compatibility within copolymer molecules where the mixing within the molecule is fixed by the synthesis. In most cases the molecules are not altered during phase changes, unless the molecules have a dynamic structure as, for example, caused by transesterification and transamidation. As long as the sequences of repeating units of the different components within the copolymers are short, possible exothermic heats of solution are commonly insufficient to overcome the entropic driving force for mixing of the sequences between different molecules and compatibility (solubility) results, as shown in Figure 12. As the sequences get sufficiently longer, phase separation occurs and molecular segments undergo

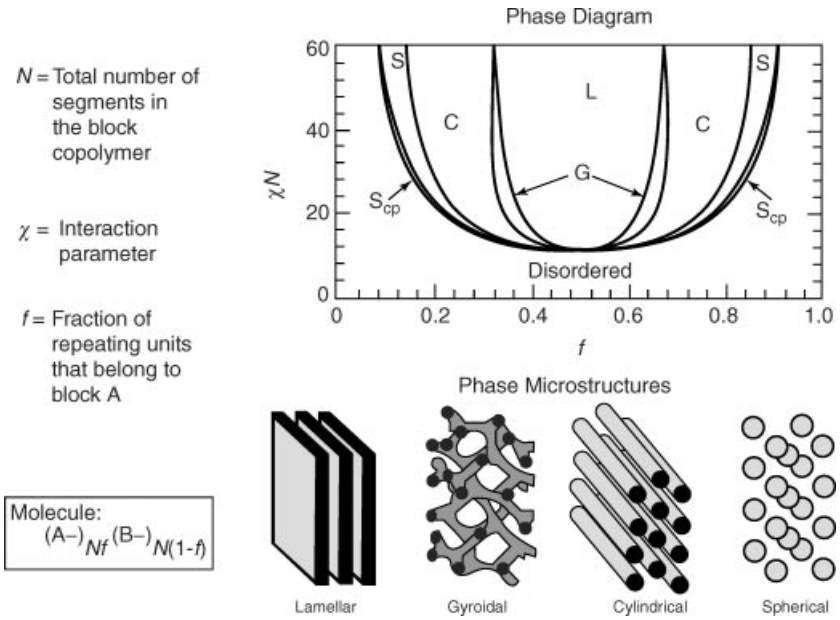

Fig. 12. Phase diagram and phase microstructures for block copolymers. The areas L, G, C, and S correspond to the structures sketched at the bottom; S_{cp} represents more complicated structures (112).

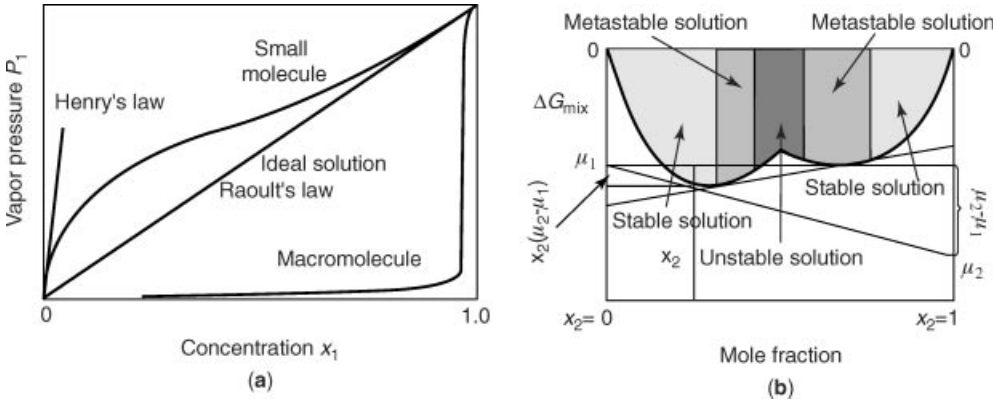

Fig. 13. Vapor pressure P_1 of and free enthalpy of mixing $[\Delta G_{mix} = \mu_1 + x_2\,(\mu_2 - \mu_1)]$ for solutions of components 1 and 2.

decoupling within the molecule, now usually called a block copolymer. Since the decoupled molecular segments must cross the phase boundary at the points of decoupling, special microphase structures arise which produce a minimum in interfacial energy, as shown in Figure 12 (112,113).

The temperature of the transition between two different phase structures is thermodynamically defined by the equality of their partial molar free enthalpies μ_1 and μ_2. Figure 13**a** illustrates the so-called ideal solution in a plot of the vapor pressure P_1 as a function of concentration in terms of the mole fraction x_1 (Raoult's law, $x_1\,P_0 = P_1$, where P_0 is the vapor pressure of the pure solvent 1). In this ideal case, only the entropy of mixing, $\Delta S_1 = -RT \ln x_1$, changes the chemical potential of the solvent, ${\mu_1}^s$, from its pure state, ${\mu_1}^0$, as expressed by

$$\mu_1^s = \mu_1^0 + RT \ln x_1 \tag{35}$$

Note that x_1 is smaller than 1, causing the positive entropy and negative contribution to the chemical potential stabilizing the solution. The vapor pressure lowering and other colligative properties are used to determine molecular masses of the solute 2.

A more quantitative treatment must also consider the change in enthalpy on mixing. The solubility parameter δ as defined as

$$\delta = (\Delta E_{vap}/V)^{1/2} \tag{36}$$

where ΔE_{vap} is the energy of evaporation to a gas at zero pressure and V is the molar volume. If there are no specific forces such as strongly polar groups, hydrogen bonds, or largely different geometries in solution and pure components, the enthalpy of mixing per unit volume is given by

$$\Delta h = v_1 v_2 (\delta_1 - \delta_2)^2 \tag{37}$$

where v_1 and v_2 are the volume fractions of the two components. Since the overall thermodynamic stability relative to the pure states must be negative for a stable

solution, the positive value of equation 37 must be overcome by the increase in entropy of mixing as shown by equation 35. Figure 13**a** displays the effect of a positive heat of mixing on the with the upper bold line. The vapor pressure of the solvent is increased and approaches the pure solute concentration ($x_1 = 0$) with the Henry's law slope which is usually accounted for by introducing an activity a_1 in place of the mole fraction x_1 ($a_1 {P_1}^0 = P_1$). For quantitative vapor pressure measurement, the approach to Raoult's law for dilute solutions is applicable, even in the presence of an enthalpy of interaction. For macromolecules, another deviation from Raoult's law must be accounted for the large size of the macromolecule. For macromolecules, a_1, the activity of the low molar mass solvent, is close to zero for most of the concentration range before it approaches Raoult's law; ie, a large mole fraction dissolves in a polymer melt without resulting in noticeable vapor pressure. Perhaps, this should not be surprising if one remembers that x_1 must be large compared to x_2 to achieve comparable masses for the two components. The Flory–Huggins equation (114–118), to be described next, will resolve this problem and describes the vapor pressure in Figure 13**a** for cases such as natural rubber dissolved in benzene.

The first step is to describe an ideal entropy of mixing for the polymer solute neglecting any interaction energy

$$\mu_2^s - \mu_2^o = RT[\ln v_2 + (1-x)(1-v_2)] \tag{38}$$

where v_2 and $v_1 = (1 - v_2)$ are the volume fractions replacing the mole fractions x_2 and x_1. This expression was derived by placing the solution on a lattice with molecules 1 occupying one unit cell each, and the macromolecules using x unit cells ($x = V_2/V_1$). Note that with $x = 1$, ie, for equal sizes of both components, the equation describing the mixing reverts back to Raoults law ($v_2 = x_2$, $v_1 = x_1$). Another, easier, derivation of equation 37 is given by Hildebrand (119). He assumes that ideal liquids have a universal free volume fraction v_f. On mixing, the molecules expand as in an ideal gas. They change from the free volumes in the pure states, $V_{f1} = V_1 v_f$ and $V_{f2} = V_2 v_f$, to the total free volume $V_{f1,2} = V_{total} v_f$, also described by equation 38. For real solutions the enthalpic contribution, as described by equation 37, must be added to equation 38. Since, however, any change in interaction will also disturb the ideal entropy of mixing, a new interaction parameter χ is defined per lattice unit cell in terms of a free enthalpy instead of an enthalpy parameter

$$\mu_2^s - \mu_2^o = RT\left[\ln v_2 + (1-x)(1-v_2) + \chi x (1-v_2)^2\right] \tag{39}$$

Figure 13**b** illustrates, then, the change of the free enthalpy of mixing by adding the appropriate chemical potentials of the components as suggested by equation 32. The interaction term χ produces the deviation in the free enthalpy of mixing which permits two concentrations to yield the same chemical potential, as indicated. These two concentrations are equally stable and may phase separate. A further increase in concentration on the left, or decrease on the right, however, still yields a decrease in chemical potential, though less than a phase separation would. This change in free enthalpy of mixing continues until the points of inflection of the curve of the free enthalpy of mixing are reached. At these points further changes in

concentrations cause an increase in free enthalpy of mixing, making the solution unstable and causing a spontaneous, spinodal decomposition into two phases.

For a multicomponent system where all components are macromolecules, a single phase is rarely found, since ΔS becomes much smaller for large molecular sizes. The positive enthalpy of mixing of equations 37 and 39, which is more closely proportional to the number of repeating units than the number of total molecules, usually overcompensates the entropy term of equations 35 and 38 and prohibits solution. Generally speaking, macromolecules are miscible in a multicomponent system only when they are of low molecular mass or are block copolymers as shown in Figure 12, because they are very similar chemically and physically, or because of specific interactions causing a negative ΔH. A large percentage of single-phase multicomponent systems that are of practical use belong to the last group. A table of many small molecule solvents of macromolecules is given in Reference 120. Compatible polymer systems are listed in References 121 and 122. An example of a phase diagram of polystyrene dissolved in acetone for two different molar masses is shown in Figure 14 (123). Because of the change of the interaction parameter of equation 39 with temperature, an upper critical solution temperature (UCST), as well as a lower critical solution temperature (LCST), is observed, with intermediate behavior at higher molar mass.

Glassy Multicomponent Systems. In the glassy states of single-phase, multicomponent systems, only a single glass transition is possible at the temperature where the large-scale motion freezes. A special observation is that a solution

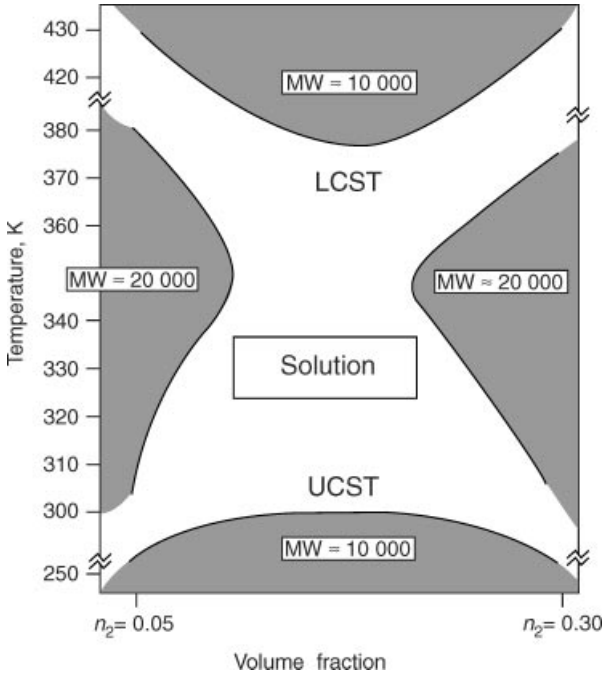

Fig. 14. Phase diagram of polystyrene in acetone, illustrating the development of an LCST and UCST by changing the molar mass.

of two small molecules or within a homogeneous copolymer system shows little change in the breadth of the glass transition, as defined in Figure 9, when compared to the pure components. If, however, one or more of the components of the solution are macromolecules, the temperature region of the glass transition is considerably broadened. This effect must be caused by the inability of the macromolecules to fully mix. Along the molecule, the arrangement of the repeating units remains unchanged on dissolution and causes nanophase regions of unmixed repeating units. Little knowledge about this effect exists beyond the experimental observation of the broadening of the glass transition (124).

The effect of composition on the glass-transition temperature $T_g(w)$ of a two-component, one-phase system has been described empirically (125) as

$$T_g(w) = wT_{g_1} + (1-w)T_{g_2} + w(1-w)K \tag{40}$$

where w is the mass fraction of component one and K is an empirical parameter chosen for good fit over the whole concentration range. Another empirical equation, the Gordon–Taylor equation, makes use of the adjustable parameter L

$$T_g(w) = [wT_{g_1} + L(1-w)T_{g_2}]/[w + L(1-w)K] \tag{41}$$

Both expressions have been linked to the conformational entropy at the glass transition (126,127). A number of additional equations have been compared to the experimental data as illustrated in Figure 15. The Gibbs–Di Marzio equation,

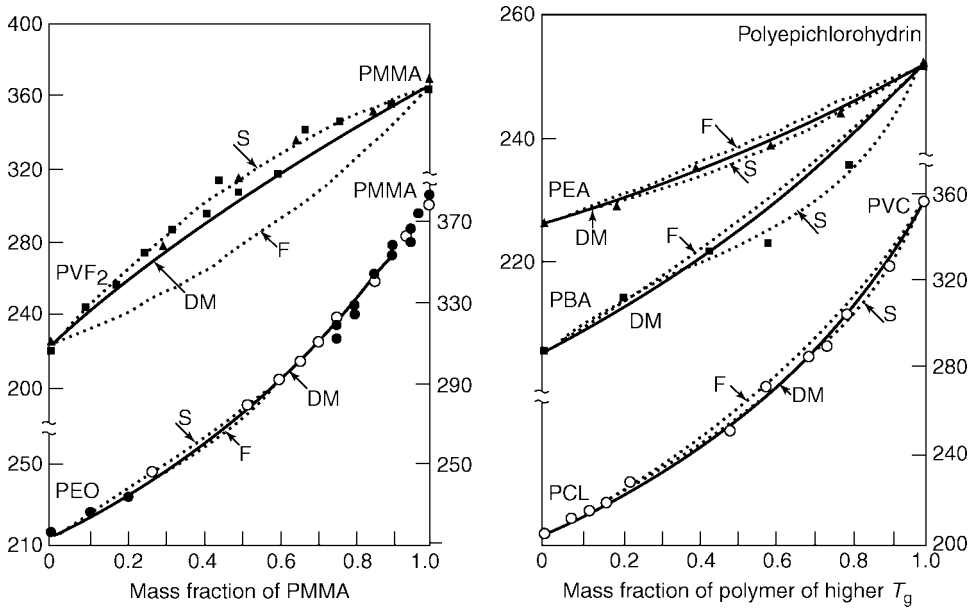

Fig. 15. Changes of the glass transition temperature for a series of polymer solutions and an effort to fit the data to equations 42 to 44. [PMMA = poly(methyl methacrylate), PVF_2 = poly(vinylidene fluoride), PEO = poly(ethylene oxide), PEA = poly(ethylene adipate), PBA = poly(butylene adipate), PVC = poly(vinyl chloride), PCL = poly(ε-caprolactone)].

abbreviated DM, is given by

$$T_g = B_1 T_{g_1} + B_2 T_{g2} \tag{42}$$

where B_1 and B_2 are the flexible bond fractions, and the Fox equation, abbreviated F, is

$$1/T_g(w) = (w/T_{g_1}) + (1-w)/T_{g_2} \tag{43}$$

Both equations are easily generalized to *PVT* equations of state assuming that the solution can be based on additivity of the homopolymer properties. The Gordon–Taylor equation, in contrast, is recovered from DM if L assumes the value $\gamma_2 w/[\gamma_1(1-w)]$ where γ represents the number of the respective flexible bonds. Finally, to add effects of specific interactions, the Gordon–Taylor equation has been expanded into a virial equation in terms of the variable w_{2c} which is the expansivity-corrected mass fraction of equation 41 [$w_{2c} = Lw_2/(w_1 + Lw_2)$]. This is the Schneider equation, S, written as

$$[T_g(w) - T_{g_1}]/[T_{g_2} - T_{g_1}] = (1+K_1)w_{2c} - (K_1+K_2)w_{2c}^2 + K_2 w_{2c}^3 \tag{44}$$

where K_1 and K_2 are the appropriate interaction constants.

Figure 15 documents that volume additivity (eq. 41) and additivity of flexible bonds (eq. 42) do not describe the data. Specific interactions as in equation 44 are needed (128). While equations 40 to 44 are often used indiscriminately for homopolymer solutions *and* copolymers, it was shown that sequence distributions in copolymers, as given by polymerization kinetics, can also be of influence on the glass transition (129,130).

Crystalline Multicomponent Systems. A multicomponent system that crystallizes with a common crystal structure is said to form mixed crystals. Formation of mixed crystals is often possible for components that crystallize in their pure state with the same crystal shapes (isomorphism). For linear macromolecules, a further condition must be fulfilled, the chain conformations of the components must match. For energy reasons, crystals usually can only be obtained with macromolecules close to their equilibrium conformations. In these conformations, close packing must be achieved with the second component, a rather rare event, although examples are known of limited solubility and cocrystallization with small molecule solvents (9).

For the more frequent case where one or more pure crystals can reach stability on cooling with the liquid solution, a eutectic phase diagram results. The free enthalpy of the pure crystal must then reach the chemical potential of its component in the solution. For equilibrium, the Flory–Huggins expression of equation 38 was used, with the free enthalpy of fusion represented by $\Delta G_f = \Delta H_f \Delta T_m / T_m{}^0$. Assuming that the molecules 2 make up the larger, macromolecular solute, one can write

$$\mu_2^s - \mu_2^0 = -\Delta G_{f_2} = -\Delta H_{f_2} \Delta T_m / T_{m_2}^0 = RT\left[\ln v_2 + (1-x)(1-v_2) + \chi x (1-v_2)^2\right] \tag{45}$$

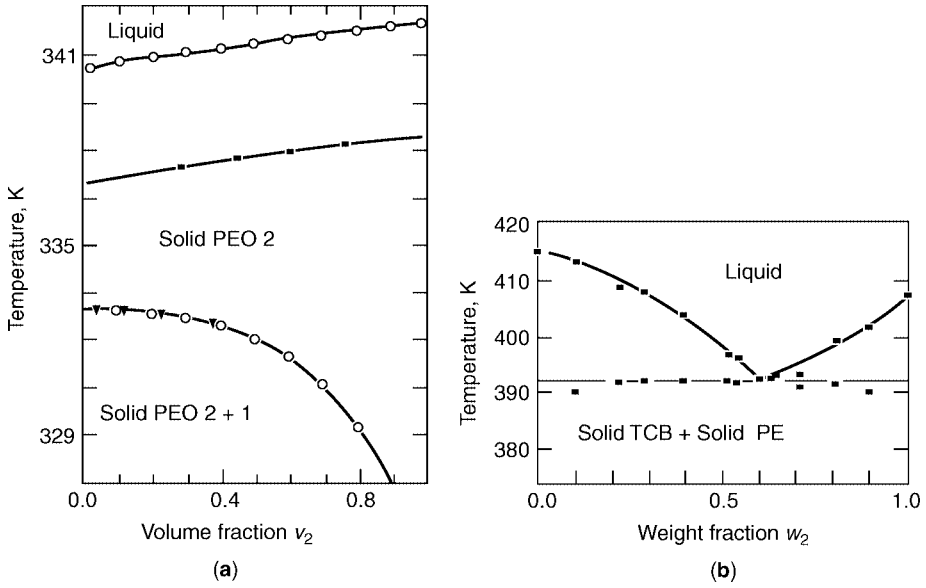

Fig. 16. (**a**) Phase diagram of poly(ethylene oxide) 3,500/100,000 mol-wt mixtures at different concentrations. The open circles represent the calculation of T_{m_2} and T_{m_1}, calculated by using the Flory–Huggins equations 46 and 47, respectively. The filled symbols represent the experimental data. (**b**) Phase diagram of polyethylene dissolved in 1,2,4,5-tetrachlorobenzene (TCB). The experimental data were obtained by melting after crystallization. The macromolecular crystals, 2, were not at equilibrium, but melted considerably lower than $T^0_{m_2}$ (see Table 1).

which can be rearranged to

$$\Delta T_{m_2} = \left[-RT^0_{m_2}/\Delta H_{f_2} \right] \left[\ln v_2 + (1-x)(1-v_2) + \chi x (1-v_2)^2 \right] \tag{46}$$

and for the smaller solvent molecule 1, an analogous expression can be derived

$$\Delta T_{m_1} = \left[-RT^0_{m_1}/\Delta H_{f_1} \right] \left[\ln v_1 + (1-\{1/x\})(1-v_1) + \chi (1-v_1)^2 \right] \tag{47}$$

Figure 16**a** is a comparison of the calculated two branches of the eutectic phase diagram for a high and a low molar mass poly(ethylene oxide). The high molarmass curve shows only a small decrease in the melting temperature with decreasing volume fraction v_2 until the logarithmic term in equation 46 forces an approach to the eutectic temperature close to the melting temperature $T^0_{m_1}$. The experimental data show a strong deviation from equation 46 for the macromolecule because of nonequilibrium effect, mainly caused by chain folding (131).

An experimental phase diagram of polyethylene dissolved in 1,2,4,5-tetrachlorobenzene (TCB) is shown in Figure 16**b** (132). Both polymer and low molar mass solvent have similar equilibrium melting temperatures. On the left-hand side of the phase diagram, the liquidus line follows equation 47, the right-hand side does not follow equation 46. Again, this indicates the usual nonequilibrium state of polymer crystals. Besides too low melting temperatures, low

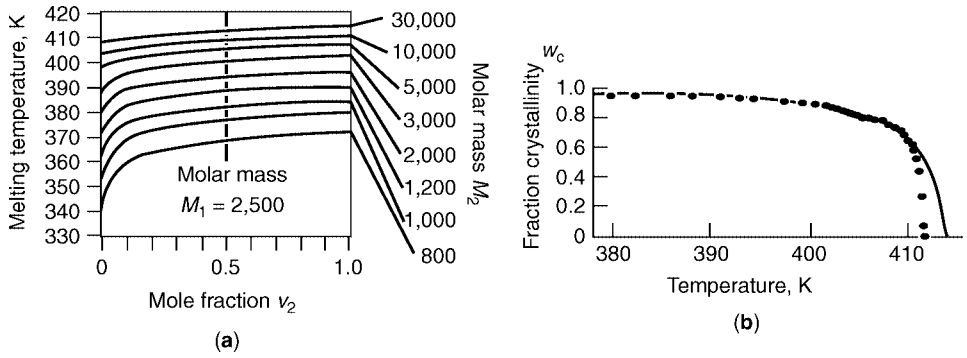

Fig. 17. (**a**) Equilibrium phase diagrams of the given molar masses of polyethylene in a low molar mass solvent of $M_1 = 2500$. (**b**) The experiments (filled circles) and the calculated crystallinities for a polyethylene of number-average molar mass of 8500 Da and a mass average molar mass of 153,300 Da.

crystallinities also are usually seen. Other complications are the presence of a rigid amorphous fraction as mentioned above in connection with the description of the pure crystals, and also the restrictions of equilibrium mixing and demixing required during melting and crystallization. If the latter processes occur too slowly, the melting or crystallization may decouple from the mixing or demixing and nonequilibrium structures may arise. An example of the change of the phase diagram because of partial decoupling of the processes during crystallization is illustrated in Figure 17. The samples were crystallized at elevated pressure to attain almost 100% crystallinity, but equilibrium, eutectically separated extended-chain crystals of the broad molar mass distribution, describable with the multicomponent form of equation 46, are seen only to the first third of melting (95). At higher temperatures, nonequilibrium mixed crystals of lower T_{m_2} are observed.

Crystallization with phase separation of random copolymers is much more complicated because usually only one component crystallizes. This component restricts the mobility of the second component to such a degree that it cannot crystallize at all. In theory, the types of phase diagrams detailed above (eutectic systems and solid solutions) should also exist for the copolymers. However, the different repeating units are connected by covalent bonds; the size effect outweighs the possible effect of demixing (11). Only local, metastable equilibrium may be achieved. The basic two-phase equilibrium theory of crystallization and melting of copolymers was developed by Flory (133). It contains the stringent condition that all crystallizable repeating units (A units) are freely available to add to crystals A. No other units can be included in the crystal of A (no isomorphism). The noncrystallizable repeating units (B units) can thus at best be located at the A crystal surface (outside the crystal proper). A general review of the earlier work is given in Reference 134. The kinetics of crystallization for copolymers is described in (135,136). Progress since then has been slow, and further work on the melting of copolymers is urgently needed. No tabular data of value can be given at present. Recent progress reports are available (137,138).

Thermodynamics of Polymer Reactions

Thermodynamics is, similarly, well suited for the description of processes which lead to changes of the molecular structure, as just seen for phase changes. A reaction with unfavorable thermodynamics expressed by a positive ΔG does not occur. However, with a negative ΔG, a reaction may still fail kinetically, while another mechanism may succeed. A typical example is the preparation of polypropylene. Although the polymerization of propylene is possible thermodynamically, it was not achieved until the work of Ziegler (139) and Natta (140), who discovered the catalyzed mechanism with favorable kinetics. Thus, much effort has been devoted to understand the kinetics of polymerization (118). Early work concentrated on predicting molecular masses and their distribution. In this section the thermodynamics of polymerization is briefly discussed. Most attention is paid to addition (chain) polymerization, but the theory is also applicable to condensation (stepwise) polymerization. The subject is extensively reviewed (141–145).

A chemical or physical reaction can only occur if there is a decrease in the free enthalpy, as discussed above. In most polymerization reactions, the entropy decreases because the polymer lacks translational and rotational motion. It has been argued that the loss of the rotational entropy is balanced by the gain of internal rotational and vibrational entropy in the polymer, and that the total loss is, therefore, equal to the translational entropy of the monomer (146). Thus, since the entropic contribution to ΔG is positive, the enthalpy of polymerization must be negative and more than compensate for the entropic term for the reaction to occur. Indeed, polymerizations are typically exothermic reactions. Polycondensations are usually acid–base type reactions that are exothermic. Addition polymerizations occur typically with the creation of two single bonds from one double bond. The bond strength of two single bonds is, however, always higher than that of one double bond; hence, those reactions are also exothermic. From the increasingly negative entropic contribution to ΔG with temperature, it follows that above a certain temperature ΔG becomes greater than zero and polymerization is no longer possible. Instead, the equilibrium of the polymerization reaction is shifted toward the monomer and a depolymerization reaction occurs. The temperature at which ΔG is zero is called the *ceiling temperature*, and is a characteristic of a polymerization reaction. It depends on the pressure of the reactant and obeys a Clausius–Clapeyron-type relation (143). Polymerizations are typically accompanied by a decrease in the system volume; thus, an increase in pressure raises the ceiling temperature. It also follows that higher pressures increase the yield of the reaction.

In some special cases, however, the polymerization is an endothermic reaction (positive ΔH) compensated by an increase in entropy. Such a case is the polymerization of elemental, eight-membered, cyclic sulfur, S_8 (147). It follows that, in such a polymerization, a minimum temperature exists below which polymerization is not possible and an inverse ceiling temperature, a floor temperature, exists. This situation can also occur in ring-opening polymerizations, where a priori predictions of the signs in ΔS and ΔH are not possible (148).

The qualitative discussion can be quantified for the prediction of the extent of a polymerization reaction.

In addition or chain polymerization, the reaction can be represented as

$$M_n^* + M_1 \rightleftarrows M_{n+1}^* \tag{48}$$

where $M_n{}^*$ is the growing chain and M_1 the monomer. The species $M_n{}^*$ and $M^*{}_{n+1}$ are indistinguishable and, therefore, the equilibrium constant is

$$K_e = \frac{\left[M_{n+1}^*\right]_e}{\left[M_n^*\right]_e [M_1]_e} \approx [M_1]_e^{-1} \tag{49}$$

The equilibrium constant K_e is equal to the free-enthalpy change $\Delta G = -RT \ln K_e$, so that

$$\ln[M_1]_e = \Delta H/(RT) - \Delta S/R \tag{50}$$

or in differential form

$$\mathrm{d}\ln[M_1]_e/\mathrm{d}T = \Delta H/(RT)^2 \tag{51}$$

where $[M_1]$ is the chemical activity of the monomer, which, in a first approximation, equals its concentration. The concentration $[M_1]_e$ is the equilibrium monomer concentration at the ceiling temperature. For the polymerization to proceed, the monomer concentration $[M_1]$ must be higher than $[M_1]_e$. For lower concentrations, depolymerization occurs.

In step polymerization, the reaction can be represented as

$$\mathrm{A} + \mathrm{B} \rightleftarrows \mathrm{C} + \mathrm{D} \tag{52}$$

where A and B are the reacting species. The species in an esterification are —OH and —COOH, and C is the resulting polymer, a polyester, and D is the by-product, H_2O. The reaction constant is $K = [\mathrm{C}][\mathrm{D}]/([\mathrm{A}][\mathrm{B}])$. For the reaction to occur, K must be smaller than the equilibrium constant K_e. This is usually forced by removing the by-product D from the system.

From the above discussion, the importance of the knowledge of ΔH and ΔS, and therefore ΔG for polymerization reactions, is obvious. The enthalpy and entropy of some polymerization reactions are given in Table 5. The experimental methods for their determination have been reviewed (141,149,150). For the determination of the entropy, the direct method is based on equation 50. From a plot of the equilibrium concentration of the monomer vs $1/T$, both ΔH and ΔS can be computed. Another method involves the estimation of ΔS from kinetic frequency factors (146).

In most cases, however, the change in enthalpy and entropy are calculated from the difference between the enthalpies (heats) of formation and entropies of formation of the products (polymer) and the reactants (monomer). Naturally, to do so, both the enthalpy and entropy of the polymer and the monomer must be known. The heat of formation of a substance which can be produced by direct reaction of its elements is the heat of the reaction, but only very few and simple substances can be formed directly from their elements. Therefore, experimentally, the heat

Table 5. Heats and Entropies of Polymerization[a]

Monomer	State[b]	ΔH, kJ/mol	ΔS, J/(K · mol)	T^c, K	Comments
Ethylene	g,g[d]	93.5	142	298	
	g,c	101.5	155 (158)[e]	298	
	g,c′	108.5 (107.5)[e]	172 (174)[e]	298	
Propylene	g,g	86.5	167	298	
	g,c′	104	191	298	syndiotactic
	g,c′	104	205	298	isotactic
	l,c	84	113 (116)[e]	298	various tacticities
	l,c′		136	298	isotactic 100% crystalline
	s,c	69		195	in *n*–butane
1–Butene	g,g	86.5	166	298	
	l,c	83.5	113 (112)[e]	298	isotactic
Isobutylene	g,c	72		298	
	g,g		172	298	
	l,c	48	112 (121)[e]	298	
Isoprene	l,c	75	101	298	
1,3-Butadiene	g,g	73		298	1,2-polymer
	g,g	78		298	1,4-polymer
	l,c	73	89 (84)[e]	298	corrected for end groups
Styrene	g,g	74.5	149	298	
	l,c	70 (68,73)[e]	104 (105,112)[e]	298	
Tetrafluoroethylene	g,g	155		298	
	g,c′	172	197	197	ΔH at 298 K
	l,c′	163 ± 17	112	197	ΔH at 298 K
Vinyl chloride	g,c	132		298	
	l,c	96		348	$\Delta H = 71$ at 298 K
Vinylidene chloride	l,c′	75.5	89	200	ΔH at 298 K
Formaldehyde	g,c′	55 (66)[e]	169 (174)[e]		298
Acetaldehyde	l,c′	64.5		298	to poly(vinyl alcohol)
	l,c	62.5		298	to poly(vinyl alcohol)
Acetone	g,g	−12		298	
	g,c	10	188		298
Trioxane	g,g	64	298		
	c′,c′	4.5 to 11.5[e]	18 ± 16	298	in various solvents
	s,c′	12.5 to 21.5[e]	42	303	ΔS at 298 K in nitrobenzene
Ethylene oxide	g,c′	140 (127.3)[e]	174	298	ΔS for 100% cryst.
Acrylic acid	l,c	67		348	
Acrylonitrile	l,c′	76.5	109	348	ΔS at 298 K
Methacrylic acid	l,c	42.5		347	$\Delta H = 64.5$ at 298 K
Methyl methacrylate	l,c	56	117	400	ΔH at 403 K
Vinyl acetate	l,c	88		348	

[a] Extracted from the extensive tables of W. K. Busfield, in Ref. 120, pp. II. 295–334.

[b] State of the monomer (first letter) and of polymer (second letter); g = gas (hypothetical for polymer), l = liquid, c = glassy condensed phase, c′ = crystalline or partially crystalline condensed phase, and s = solultion in the specified solvent.

[c] Temperature where ΔH and ΔS were measured or corrected to.

[d] The gaseous state is hypothetical; $\Delta H_{g,g}$ and $\Delta S_{g,g}$ were calculated from semiempirical schemes and correspond to the experiment only after correction with the sublimation enthalpy and entropy of the polymer.

[e] When several values are available, a second or third value is given in parentheses; for more measurements the range is indicated.

of formation of an organic substance is usually found indirectly through heats of combustion. In such an experiment, the substance is burned in an autoclave and the heat of combustion is measured. From the heat of combustion and the known heats of formation of the products, the heat of formation can be calculated. Details are given in physical chemistry textbooks (151).

The entropy of formation of a substance can be found from calorimetric measurements of the heat capacity from 0 K to the temperature of measurement, as outlined in equation 12. The entropy of formation is then simply the difference of the entropy of the substance and that of the constituent elements. The heat of formation and the entropy of various substances are given in standard thermodynamic tables at 298.15 K. It is often assumed that, at about room temperature, the heat and entropy of formation do not depend strongly on temperature; however, this is a misconception. The dependence of these quantities on temperature is evident from equations 11 and 12. The heats of formation, entropies, and other useful thermodynamic quantities are found in a number of standard data sources (1–7,152–157).

The enthalpy and entropy of formation of a compound can also be calculated with the help of various semiempirical addition schemes. In such schemes, each chemical bond is associated with a characteristic energy, transferable from one substance to another. The sum of the energy of the bonds of a compound is corrected for nonbonding interactions, such as stabilization due to resonance or destabilization due to steric hindrance, etc, to yield the heat of formation (158). In other schemes, no corrective terms are implied, but the number of the tabulated bonds is much higher. In this case, the results are more accurate (159). For the calculation of the entropy of formation, a similar method was applied, but here the entropy contributions of whole chemical groups were tabulated (160). More information on such schemes as applied to polymers and monomers is given in References 161–163. These semiempirical methods give the heat (and entropy) of formation of the compound in its gaseous state. The resulting data must be corrected by subtracting the enthalpy (and entropy) of vaporization for liquids, or of sublimation (vaporization and fusion) for solids. In Table 5 the states of the monomer and polymer are given. A gaseous polymer is, of course, hypothetical. In several cases the enthalpy and entropy of polymerization were calculated for both the polymer and monomer in the gaseous state. Correction according to the previous rules is then necessary.

BIBLIOGRAPHY

"Thermodynamic Properties" in *EPST* 1st ed., Vol. 13, pp. 788–831, by R. M. Joshi, National Chemical Laboratory, India; in *EPST* 2nd ed., Vol. 13, pp. 767–807, by B. Wunderlich, S. Z. D. Cheng, and K. Loufakis, Oak Ridge National Laboratory and The University of Tennessee, Knoxville.

1. Landolt-Boernstein, *Zahlenwerte und Funktionen*, 6th ed., Vol. 2, Parts 1–5, Springer-Verlag, Berlin, 1956–1971; continued as K. H. Hellwege, ed., *Macroscopic and Technical Properties of Matter*, neue Serie, Group IV.
2. Thermodynamics Research Center Data Project, *Selected Values of Properties of Chemical Compounds*, 4 vols., Texas A&M University, College Station, Tex., 1985.

3. American Petroleum Institute Research Project 44, *Selected Values of Properties of Hydrocarbon and Related Compounds*, Thermodynamics Research Center, Texas A&M University, College Station, Tex., 1986.
4. Y. S. Touloukian and C. Y. Ho, eds., Thermodynamical Properties of Matter, The TPRC Data Series, IFI/Plenum, New York, 1970–1979.
5. M. Kh. Karapet'yants and M. L. Karapet'yants, *Thermodynamic Constants of Inorganic and Organic Compounds* (translated by J. Sehmork) Humphrey Science Publishers, Ann Arbor, Mich., 1970.
6. I. Barin and O. Knacke, *Thermochemical Properties of Inorganic Substances*, Springer Verlag, Berlin, 1973, Suppl. 1977.
7. D. R. Lide Jr., ed. *CRC Handbook of Chemistry and Physics*, CRC Press, Boca Raton, Fla, annual editions.
8. B. Wunderlich, *Prog. Polym. Sci.* **28**, 383 (2003).
9. B. Wunderlich, *Macromolecular Physics, Vol. 1: Crystal Structure, Morphology, Defects*, Academic Press, New York, 1973.
10. B. Wunderlich, *Macromolecular Physics, Vol. 2: Crystal Nucleation, Growth, Annealing*, Academic Press, New York, 1976.
11. B. Wunderlich, *Macromolecular Physics, Vol. 3: Crystal Melting*, Academic Press, New York, 1980.
12. B. Wunderlich and J. Grebowicz, *Adv. Polym. Sci.* **60/61**, 1 (1984); see also other articles on liquid crystals in *Adv. Polym. Sci.* **59–61** (1984).
13. B. Wunderlich, M. Moeller, J. Grebowicz, and H. Baur, *Conformational Motion and Disorder in Low and High Molecular Mass Crystals*, (Advances in Polymer Science 87), Springer, Berlin, 1988.
14. W. W. Wendlandt, *Thermal Analysis*, 3rd ed., John Wiley & Sons, Inc., New York, 1986.
15. W. Hemminger and W. Höhne, *Calorimetry, Fundamentals and Practice*, Verlag Chemie, Weinheim, Germany, 1984.
16. C. J. Keattch, *An Introduction to Thermogravimetry*, Heyden and Son, London, 1975.
17. A. Weissberger and B. Rossiter, eds., *Physical Methods of Chemistry*, Vol. 1, Part V, Wiley-Interscience, New York, 1971.
18. E. Mueller, *Physikalische Methoden, Vol 3: Methoden der Organischen Chemie (Houben-Weyl)*. Part 1, G. Thieme, Stuttgart, Germany, 1955.
19. J. M. Sturtevant, in Ref. 17.
20. W. P. White, *The Modern Calorimeter*, Chemical Catalog Co., New York, 1928.
21. J. P. McCullogh, *Chemical Thermodynamics, Vol. 1: Calorimetry of Nonreacting Systems*, Plenum Press, New York, 1968.
22. B. Wunderlich, *Thermal Analysis*, Academic Press, New York, 1990.
23. G. Höhne, W. Hemminger, and H.-J. Flammersheim, *Differential Scanning Calorimetry*, Springer, Berlin, 1996, 2nd ed. 2003.
24. F. D. Rossini and H. A. Skinner, eds., *Experimental "Thermochemistry'*, Vols. 1 and 2, Interscience Publishers, New York, 1956, 1962; H. Weber, *Isothermal Calorimetry*, H. Lang and P. Lang, Bern and Frankfurt, 1973.
25. *Proceedings of the International Conferences on Thermal Analysis (and Calorimetry)* can be found under the title *Thermal Analysis*, various publications and editions., 1965, 1969, 1972, 1975, 1977, 1980, 1982, and later published in *Thermochim. Acta* **92/93** (1985), **133/135** (1988), and *J. Therm. Anal*. **40** (1993), **49** (1997), **64** (2001).
26. Proceedings of the North American Thermal Analysis Society, annual editions, since 2003 on CD-ROM.
27. Chemical Abstract Service of the Am. Chem. Soc., *Sections on Thermal Analysis*, #03B, Columbus, Ohio.
28. E. A. Turi, ed., *Thermal Characterization of Polymeric Materials*, Academic Press, New York, 1981; 2nd ed. 1997.

29. B. Wunderlich, in S. Z. D. Cheng, ed., *Handbook of Thermal Analysis and Calorimetry, Vol. 3: Applications to Polymers and Plastics*, Elsevier Science, Amsterdam, 2002, pp. 1–47.
30. J. Pak and B. Wunderlich, *Thermochim. Acta* **367/368**, 229 (2001).
31. H. Baur and B. Wunderlich, *Adv. Polym. Sci.* **7**, 151 (1970).
32. H. S. Bu, S. Z. D. Cheng, and B. Wunderlich, *J. Phys. Chem.* **91**, 4179 (1987).
33. B. Wunderlich, *Pure Appl. Chem.* **67**, 1019 (1995).
34. ATHAS Data Bank.web.utk.edu/∼athas/
35. U. Gaur, H.-C. Shu, A. Mehta, and B. Wunderlich, *J. Phys. Chem. Ref. Data* **10**, 89 (1981).
36. U. Gaur and B. Wunderlich, *J. Phys. Chem. Ref. Data* **10**, 119 (1981).
37. U. Gaur and B. Wunderlich, *J. Phys. Chem. Ref. Data* **10**, 1001 (1981).
38. U. Gaur and B. Wunderlich, *J. Phys. Chem. Ref. Data* **10**, 1051 (1981).
39. U. Gaur and B. Wunderlich, *J. Phys. Chem. Ref. Data* **11**, 313 (1982).
40. U. Gaur, S.-F. Lau, B. B. Wunderlich, and B. Wunderlich, *J. Phys. Chem. Ref. Data* **11**, 1065 (1982).
41. U. Gaur, B. B. Wunderlich, and B. Wunderlich, *J. Phys. Chem. Ref. Data* **12**, 29 (1983).
42. U. Gaur, S.-F. Lau, B. B. Wunderlich, and B. Wunderlich, *J. Phys. Chem. Ref. Data* **12**, 65 (1983).
43. U. Gaur, S.-F. Lau and B. Wunderlich, *J. Phys. Chem. Ref. Data* **12**, 91 (1983).
44. M. Varma-Nair and B. Wunderlich, *J. Phys. Chem.* **20**, 349 (1991).
45. H. S. Bu, W. Aycock, and B. Wunderlich, *Polymer* **28**, 1165 (1987).
46. J. Grebowicz, W. Aycock, and B. Wunderlich, *Polymer* **27**, 575 (1986).
47. S.-F. Lau, H. Suzuki, and B. Wunderlich, *J. Polym. Sci. Polym. Phys. Ed.* **22**, 379 (1984).
48. L. H. Judovits, Ph.D. dissertation, Rensselaer Polytechnic Institute, Troy, N.Y., 1985.
49. L. H. Judovits, R. C. Bopp, U. Gaur, and B. Wunderlich, *J. Polym. Sci., Polym. Phys. Ed.* **24**, 2725 (1986).
50. A. Xenopoulos, K. Roles, and B. Wunderlich, *Polymer* **34**, 2559 (1993).
51. D. E. Kirkpatrick and B. Wunderlich, *Makromol. Chem.* **186**, 2595 (1985).
52. S. Z. D. Cheng and B. Wunderlich, *Macromolecules* **20**, 1630 (1987).
53. S. Z. D. Cheng, R. Pan R, and B. Wunderlich, *Makromol. Chem.* **189**, 2443 (1988).
54. M.-Y. Cao, M. Varma-Nair, and B. Wunderlich, *Polym. Adv. Technol.* **1**, 151 (1990).
55. S. Z. D. Cheng, M.-Y. Cao, and B. Wunderlich, *Macromolecules* **19**, 1868 (1986).
56. M. Varma-Nair, Y. Jin, J. Cheng, and B. Wunderlich, *Macromolecules* **24**, 5442 (1991).
57. M. Varma-Nair, J. P. Wesson, and B. Wunderlich, *J. Therm. Anal.* **35**, 1913 (1989).
58. *Einstein Function Table, National Bureau of Standards Monograph 49*, National Bureau of Standards, Washington, D.C., 1962.
59. J. A. Beattie, *J. Math. Phys. (MIT)* **6**, 1 (1926–1927).
60. U. Gaur, G. Pultz, H. Wiedemeier, and B. Wunderlich, *J. Therm. Anal.* **43**, 297 (1981).
61. B. Wunderlich, *J. Chem. Phys.* **37**, 1207 (1962).
62. V. V. Tarasov, *Zh. Fiz. Khim.* **24**, 1430 (1953); **39**, 2077 (1965); *Dokl. Akad. Nauk.*, SSSR **100**, 307 (1955).
63. S. Z. D. Cheng, S. Lim, L. H. Judovits, and B. Wunderlich, *Polymer* **28**, 10 (1987).
64. K. Loufakis and B. Wunderlich, *Polymer* **26**, 1875 (1985); **27**, 563 (1986).
65. R. Pan, M. Varma, and B. Wunderlich, *J. Therm. Anal.* **35**, 955 (1989).
66. J. Grebowicz and B. Wunderlich, *J. Therm. Anal.* **30**, 227 (1985).
67. I. Okazaki and B. Wunderlich, *J. Polym. Sci., Part B: Polym. Phys.* **34**, 2941 (1996).
68. B. Wunderlich and I. Okazaki, *J. Therm. Anal.* **49**, 57 (1997).
69. H. Suzuki and B. Wunderlich, *Makromol. Chem.* **189**, 1109 (1985).
70. J. Pak, M. Pyda, and B. Wunderlich, *Macromolecules* **36**, 495 (2003).
71. B. Wunderlich, *J. Chem. Phys.* **29**, 1395 (1958).
72. K. Loufakis and B. Wunderlich, *J. Phys. Chem.* **92**, 4205 (1988).

73. M. Pyda and B. Wunderlich, *Macromolecules* **32**, 2044 (1999).
74. P. H.-C. Shu, U. Gaur, and B. Wunderlich, *J. Polym. Sci., Polym. Phys. Ed.* **18**, 449 (1980).
75. H. Suzuki and B. Wunderlich, *J. Polym. Sci., Polym. Phys. Ed.* **23**, 1671 (1985).
76. S. Z. D. Cheng, R. Pan, H. S. Bu, M.-Y. Cao, and B. Wunderlich, *Makromol. Chem.* **189**, 1579 (1988).
77. S. Z. D. Cheng and B. Wunderlich, *J. Polym. Sci., Polym. Phys. Ed.* **24**, 1755 (1986).
78. R. Simha and T. Somcynsky, *Macromolecules* **2**, 342 (1969).
79. R. Simha, *Macromolecules* **10**, 1025 (1977).
80. O. Olabisi and R. Simha, *Macromolecules* **8**, 211 (1975).
81. P. Zoller, *J. Appl. Polym. Sci.* **23**, 1051 (1979).
82. P. Zoller, *J. Appl. Polym. Sci.* **23**, 1057 (1979).
83. P. Zoller, *J. Appl. Polym. Sci.* **21**, 3129 (1977).
84. P. Zoller, *J. Appl. Polym. Sci.* **22**, 633 (1978).
85. P. Zoller and P. Bolli, *J. Macromol. Sci. Phys.* **1318**, 555 (1980).
86. P. Zoller, *J. Polym. Sci., Polym. Phys. Ed.* **20**, 1453 (1982).
87. L. D. Loomis and P. Zoller, *J. Polym. Sci., Polym. Phys. Ed.* **21**, 241 (1983).
88. I. C. Sanchez and R. H. Lacombe, *J. Polym. Sci., Polym. Lett. Ed.* **15**, 71 (1977).
89. I. C. Sanchez and R. H. Lacombe, *J. Phys. Chem.* **80**, 2352 (1976).
90. P. J. Flory, R. A. Orwoll, and A. Vrij, *J. Am. Chem. Soc.* **86**, 3507 (1964).
91. P. J. Flory, *Discuss. Faraday Chem. Soc.* **49**, 7 (1970).
92. P. Ehrenfest, *Proc. Acad. Sci. Amsterdam* **36**, 153 (1933).
93. A. R. Ubbelohde, *Melting and Crystal Structure*, Clarendon Press, Oxford, 1965; *The Molten State of Matter, Melting and Crystal Structure*, John Wiley & Sons. Inc., New York, 1978.
94. B. Wunderlich, *Polymer* **5**, 125 , 611(1964).
95. R. B. Prime and B. Wunderlich, *J. Polym. Sci. Polym. Phys. Ed.* **7**, 2073 (1969).
96. R. B. Prime, B. Wunderlich, and L. Melillo, *J. Polym. Sci., Polym. Phys. Ed.* **7**, 2091 (1969).
97. H. Baur, *Thermophysics of Polymers, Vol 1: Theory*, Springer, Berlin, 1999.
98. B. Wunderlich and E. Hellmuth, *J. Appl. Phys.* **36**, 3039 (1965).
99. J. D. Hoffman, *Polymer* **23**, 656 (1982); **24**, 3 (1983); **26**, 803, 1763 (1985).
100. G. Kanig, *Kolloid Z. Z. Polym.* **233**, 54 (1969).
101. S. E. B. Petri, in E. Baer and S. V. Radeliffe, eds., *Polymeric Materials: Relationships between Structure and Mechanical Behavior*, American Society of Metals, Metals Park, Ohio, 1974.
102. T. Somcynsky and R. Simha, *J. Appl. Phys.* **42**, 4545 (1971).
103. J. H. Gibbs and E. A. DiMarzio, *J. Chem. Phys.* **28**, 373 (1958).
104. G. Adam and J. H. Gibbs, *J. Chem. Phys.* **43**, 139 (1965).
105. B. Wunderlich, D. M. Bodily, and M. H. Kaplan, *J. Appl. Phys.* **35**, 95 (1964).
106. R. Boyer, *J. Macromol. Sci. Phys. B* **12**, 253 (1976).
107. M. C. Shen and A. Eisenberg, *Rubber Chem. Technol.* **43**, 59 (1970).
108. A. T. Riga and L. H. Judovits, eds., *Material Characterization by Dynamic and Modulated Thermal Analytical Techniques*, ASTM STP 1402, American Society for Testing and Materials, West Conshohocken, Pa., 2001.
109. S. Matsuoka, *Relaxation Phenomena in Polymers*, Hanser, Munich, 1992.
110. B. Wunderlich, *J. Phys. Chem.* **64**, 1052 (1960).
111. H. Suzuki and B. Wunderlich, *J. Polym. Sci., Polym. Phys. Ed.* **23**, 1671 (1985).
112. M. W. Matsen and F. S. Bates, *Macromolecules* **29**, 1091 (1996).
113. M. W. Matsen and F. S. Bates, *J. Chem. Phys.* **106**, 2436 (1997).
114. M. L. Huggins, *J. Phys. Chem.* **46**, 151 (1942).
115. M. L. Huggins, *Ann. N.Y. Acad. Sci.* **41**, 1 (1942).

116. M. L. Huggins, *J. Am. Chem. Soc.* **64**, 1712 (1942).
117. P. J. Flory, *J. Chem. Phys.* **10**, 51 (1942).
118. P. J. Flory, *Principles of Polymer Chemistry*, Cornell University Press, Ithaca, 1953.
119. J. H. Hildebrand, *J. Chem. Phys.* **15**, 225 (1947).
120. O. Fuchs, in J. Brandrup and E. H. Immergut, eds., *Polymer Handbook*, 3rd ed., Wiley-Interscience, 1989, pp. VII. 379–407.
121. S. Krause, in J. Brandrup and E. H. Immergut, eds., *Polymer Handbook*, 3rd ed., Wiley-Interscience, 1989, pp. VI. 347–370.
122. D. R. Paul and S. Newman, eds., *Polymer Blends*, Academic Press, New York, 1978.
123. K. S. Siow, D. Delmas, and D. Patterson, *Macromolecules* **5**, 29 (1972).
124. S.-F. Lau, J. Pathak, and B. Wunderlich, *Macromolecules* **15**, 1278 (1982).
125. E. Jenckel and R. Heusch, *Kolloid-Z* **130**, 89 (1958).
126. J. M. Gordon, G. B. Rouse, J. H. Gibbs, and W. M. Risen Jr., *J. Chem. Phys.* **66**, 4971 (1977).
127. H. A. Schneider, M.-J. Breckner and H.-J. Cantow, *Polym. Bull.* **14**, 479 (1985).
128. H. A. Schneider and E. A. DiMarzio, *Polymer* **33**, 3453 (1992).
129. H. Suzuki, N. Kamura, and Y. Nishio, *Polymer* **35**, 5555 (1994).
130. H. Suzuki and V. B. F. Mathot, *Macromolecules* **22**, 1380 (1989).
131. S. Z. D. Cheng and B. Wunderlich, *J. Polym. Sci., Polym. Phys. Ed.* **24**, 575 , 595(1986).
132. P. Smith and A. J. Pennings, *J. Materials Sci.* **11**, 1450 (1976).
133. P. J. Flory, *Trans. Faraday Soc.* **51**, 848 (1955).
134. L. Mandelkern, *Crystallization of Polymers*, McGraw-Hill, Inc., New York, 1964, Chapt. 4.
135. I. C. Sanchez and R. K. Eby, *J. Res. Natl. Stds.* **77A**, 353 (1973); *Macromolecules* **8**, 639 (1975).
136. E. Helfand and J. I. Lauritizan Jr. *Macromolecules* **6**, 631 (1973).
137. *Proceedings of the International Symposium on Polymer Crystallization in Mishima*, Japan, June 9–12, 2002, pp. 74–77, Partially printed in *J. Macromol. Sci. Part B : Phy. Ed*. **42**, (2003).
138. M. Dosiére, ed., *Crystallization of Polymers*, Kluver, Dordrecht, 1993.
139. K. Ziegler, E. Helzkamp, H. Breil, and H. Martin, *Angew. Chem.* **67**, 426 (1955).
140. G. Natta, P. Pine, P. Corradini, F. Danusso, E. Mantica, G. Mazzanti, and G. Moranglio, *J. Am. Chem. Soc.* **77**, 1708 (1955).
141. R. M. Joshi and B. T. Zwolinski, in G. E. Ham, ed., *Vinyl Polymerization*, Vol. 1, Part I, Marcel Dekker, New York, 1967, Chapt. 8.
142. P. C. Allen and C. R. Patrick, *Kinetics and Mechanisms of Polymerization Reactions*, John Wiley & Sons, Inc., New York, 1974.
143. K. J. Ivin, in A. D. Jenkins and A. Ledwith, eds., *Reactivity, Mechanism and Structure in Polymer Chemistry*, John Wiley & Sons, Inc., New York, 1974, Chapt. 4.
144. G. Odian, *Principles of Polymerization*, John Wiley & Sons, Inc., New York, 1981.
145. H. R. Allcock and F. W. Lampe, *Contemporary Polymer Chemistry*, Prentice-Hall, New Jersey, 1981.
146. F. S. Dainton and K. J. Ivin, *Q. Rev. (London)* **12**, 61 (1958).
147. A. Eisenberg and A. V. Tobolsky, *J. Polym. Sci.* **46**, 19 (1960); A. V. Tobolsky and A. Eisenberg, *J. Am. Chem. Soc.* **81**, 780 (1959).
148. H. R. Allcock, *Heteroatom Ring Systems and Polymers*, Academic Press, New York, 1967.
149. F. S. Dainton and K. J. Ivin, in H. A. Skinner, ed., *Experimental Thermochemistry*, Vol. 2, Wiley-Interscience, New York, 1962.
150. F. D. Rosini and S. Summer, eds., *Experimental Thermochemistry*, Vol. 3, Pergamon Press, Elmsford, N.Y., 1979.
151. P. W. Atkins, *Physical Chemistry*, 6th ed., Oxford University Press, Oxford, 1998.

152. K. Raznjeric, *Handbook of Thermodynamic Tables and Charts*, Hemisphere Publishing Co., McGraw-Hill Inc., New York, 1976.
153. R. H. Perry, ed., *Chemical Engineers' Handbook*, McGraw-Hill, Inc., New York, 1973.
154. R. C. Wilhoit and B. J. Zwolinski, *J. Phys. Chem. Ref. Data* **2**(suppl. 1) (1973).
155. Selected Values of Chemical Thermodynamic Properties, NBS Technical Notes 270-3 to 270-7, Institute for Basic Standards, National Bureau of Standards, Washington D.C., 1968–1973.
156. Consolidated Index of Selected Property Values: Phys. Chem. and Thermodynamics, National Academy of Sciences, National Research Council, Publ. 976, Washington, D.C., 1962.
157. J. Brandrup, E. H. Immergut, and E. A. Grulke EA, eds., *Polymer Handbook*, 4th rev. ed., John Wiley & Sons, Inc., New York, 1999.
158. L. Pauling, *The Nature of the Chemical Bond*, 3rd ed., Cornell University Press, Ithaca, N.Y., 1960.
159. J. D. Cox, *Tetrahedron* **19**, 1975 (1963).
160. G. J. Janz, *Estimation of Thermodynamic Properties of Organic Compounds*, Academic Press, New York, 1958.
161. F. S. Dainton and K. J. Ivin, *Trans. Faraday Soc.* **46**, 331 (1950).
162. R. M. Joshi, B. Zwolinski, and C. W. Hayes, *Macromolecules* **1**, 30 (1968).
163. O. E. Grikina, N. F. Stepanov, V. M. Tatevskii, and S. S. Yarovoi, *Vysokomol. Soedin A* **13**, 575 (1971).

BERNHARD WUNDERLICH
MAREK PYDA
University of Tennessee
Chemical Sciences Division of Oak Ridge National Laboratory

THERMOFORMING. See Volume 8.